



SINTEF Building and Infrastructure
COIN – Concrete Innovation Centre

Address: NO-7465 Trondheim
NORWAY
Location: Richard Birkelands vei 3
Telephone: +47 73 59 52 24
Fax: +47 73 59 71 36

Enterprise No.: NO 948 007 029 MVA

SINTEF REPORT

TITLE

COIN P3 Innovative construction concepts
SP 3.3 F Hybrid structures

Ice abrasion data on concrete structures – an overview

State of the art

AUTHOR(S)

Egil Møen, Stefan Jacobsen, Håvard Myhra

CLIENT(S)

Aker Kværner Engineering and Technology, Borregaard LignoTech, maxitGroup, Norcem A.S, Norwegian Public Roads Administration, Rescon Mapei AS, Spenncon AS, Unicon AS, Veidekke ASA and The Research Council of Norway

| | | | |
|----------------------------------|--------------------------------|--|---|
| REPORT NO. SBF BK A07036 | CLASSIFICATION Unrestricted | CLIENTS REF. Terje F. Rønning | |
| CLASS. THIS PAGE Unrestricted | ISBN 978-82536-1000-9 | PROJECT NO. 3D005841 | NO. OF PAGES/APPENDICES 62 |
| ELECTRONIC FILE CODE | | PROJECT MANAGER (NAME, SIGN.) Helge Brå | CHECKED BY (NAME, SIGN.) Stefan Jacobsen |
| FILE CODE | DATE 2007-12-20 For | APPROVED BY (NAME, POSITION, SIGN.) Tor Arne Hammer, Centre Manager | |

ABSTRACT

Data on ice abrasion published in the literature are presented and discussed briefly with main emphasize on concrete strength and ice properties. Most of the studies focus on either material properties (compressive strength, normal versus light weight aggregate, etc) or ice conditions (temperature, salinity, contact pressure). Some studies more or less ignore concrete material parameters, pointing to effects amplifying the damage such as increased ice pressure, confinement of ice, low temperature/hard ice, sand/grit pollution in the ice, ice-free concrete surface etc. Other studies point to a reduction in ice abrasion rate of both concrete and rock with increasing compressive strength of the tested material. Among the reviewed literature both development and conduction of lab test equipment and field studies are included. Test parameters and relation between field and lab are discussed as well as the importance of developing simple, repeatable tests limiting future studies to a practical number of material (strength, aggregate, fiber, additives) and ice-load parameters (contact pressure, temperature, loading rate, exposure mode - rotation or sliding, friction - kinetic or combined static/ kinetic).

| KEYWORDS | ENGLISH | NORWEGIAN |
|--------------------|-------------------|------------------|
| GROUP 1 | Marine technology | Marinteknikk |
| GROUP 2 | Concrete | Betong |
| SELECTED BY AUTHOR | Ice abrasion | Isabrasjon |
| | Arctic region | Arktiske strøk |
| | Literature review | Litteraturstudie |

Foreword

COIN - Concrete Innovation Centre - is one of presently 14 Centres for Research based Innovation (CRI), which is an initiative by the Research Council of Norway. The main objective for the CRIs is to enhance the capability of the business sector to innovate by focusing on long-term research based on forging close alliances between research-intensive enterprises and prominent research groups.

The vision of COIN is creation of more attractive concrete buildings and constructions. Attractiveness implies aesthetics, functionality, sustainability, energy efficiency, indoor climate, industrialized construction, improved work environment, and cost efficiency during the whole service life. The primary goal is to fulfill this vision by bringing the development a major leap forward by more fundamental understanding of the mechanisms in order to develop advanced materials, efficient construction techniques and new design concepts combined with more environmentally friendly material production.

The corporate partners are leading multinational companies in the cement and building industry and the aim of COIN is to increase their value creation and strengthen their research activities in Norway. Our over-all ambition is to establish COIN as the display window for concrete innovation in Europe.

About 25 researchers from SINTEF (host), the Norwegian University of Science and Technology - NTNU (research partner) and industry partners, 15 - 20 PhD-students, 5 - 10 MSc-students every year and a number of international guest researchers, work on presently 5 projects:

- Advanced cementing materials and admixtures
- Improved construction techniques
- Innovative construction concepts
- Operational service life design
- Energy efficiency and comfort of concrete structures

COIN has presently a budget of NOK 200 mill over 8 years (from 2007), and is financed by the Research Council of Norway (approx. 40 %), industrial partners (approx 45 %) and by SINTEF Building and Infrastructure and NTNU (in all approx 15 %). The present industrial partners are:

Aker Kværner Engineering and Technology, Borregaard LignoTech, maxitGroup, Norcem A.S, Norwegian Public Roads Administration, Rescon Mapei AS, Spenncon AS, Unicon AS and Veidekke ASA.

For more information, see www.sintef.no/coin

TABLE OF CONTENTS

| | | |
|----------|--|-----------|
| 1 | INTRODUCTION | 4 |
| 2 | ICE ABRASION ON CONCRETE STRUCTURES – THE PHENOMENON..... | 4 |
| 3 | DATA | 5 |
| 4 | LITERATURE REVIEW | 8 |
| | 4.1 Hoff (1988)..... | 8 |
| | 4.2 Nawwar and Malhotra (1988) | 16 |
| | 4.3 Itoh et al. (1988 & 94)..... | 20 |
| | 4.4 Hanada et al. (1996) | 24 |
| | 4.5 Hara et al. (1995)..... | 27 |
| | 4.6 Janson (1988) | 32 |
| | 4.7 Janson (1989) | 37 |
| | 4.8 Huovinen (1990) | 39 |
| | 4.9 Hara et al. (1995)..... | 45 |
| | 4.10 Malhotra et al. (1996)..... | 47 |
| | 4.11 Fiorio et al. (2002)..... | 50 |
| | 4.12 Fiorio (2005) | 55 |
| 5 | FINAL DISCUSSION..... | 59 |
| 6 | CONCLUSIONS | 61 |
| 7 | REFERENCES..... | 62 |

1 INTRODUCTION

For the last decades, the performance of concrete structures under severe marine environmental conditions has gained considerable attention. There are still a number of unknown factors related to design and material selection of concrete structures exposed to ice abrasion. The amounts of published data on this subject are relatively few and it is the aim of this document to collect and present some of these in terms of abrasion rates/depths, together with the material parameters of both ice and concrete. The objective is to identify the abrasion data and the differing exposure conditions as objectively as possible without going detailed into any models, in order to draw cross over conclusions with respect to wear rates and possible materials effects and to prepare for a continued study on the subject.

2 ICE ABRASION ON CONCRETE STRUCTURES – THE PHENOMENON

The sea ice properties range from sheet ice to unconsolidated pressure ridges to multi-year consolidated floes and ridges. The ice exerts its force in a variety of different modes, depending on the structure's geometry and the ice parameters involved. Failure modes differ between crushing, flexure, buckling and shear [18]. The overall force is limited by the driving force of the ice sheet behind the largest feature that can hit the structure without failing. It is observed that larger contact areas fail at lower unit forces, whereas smaller faces fail at higher unit forces due to confinement and homogeneity of the ice. Local ice forces are limited only by the crushing strength of the ice and might be increased by a factor of 3 or more compared to the uniaxial strength, due to confinement. The effective strength is also dependent on temperature, salinity, crystal orientation and strain rate. It is generally accepted that these high local unit forces will occur only over limited areas and they will decrease significantly as contact area increases. The ice movement, caused by wind, currents and thermal expansion/contraction are the fundamental driving forces behind the phenomenon of ice abrasion. In rivers, lakes and oceans where periodic ice floes occur, concrete structures such as e.g. bridge piers, guide walls, docks, lighthouses etc experience damage at or near the waterline due to impact with ice floes. Moving ice has, in extreme cases, been known to remove all of the concrete cover at or near the waterline for marine structures [12]. The fundamental mechanism behind the ice abrasion of a concrete structure is more complex than barely the force of friction between moving ice and concrete. Field investigations and laboratory tests suggest that the observed abrasion is a result of the combination of environmental causes together with the ice impact forces. The environmental deterioration is a result of cyclic freezing and thawing and is known to cause a gradually weakening of the matrix and the aggregate bond interface. In some areas like e.g. in rivers, the ice might contain grit and hence induce an even more severe abrasion condition, known as the sandpaper effect. As will be seen in the following chapters, various efforts have been made in order to examine these local forces and their abrading effect on concrete structures.

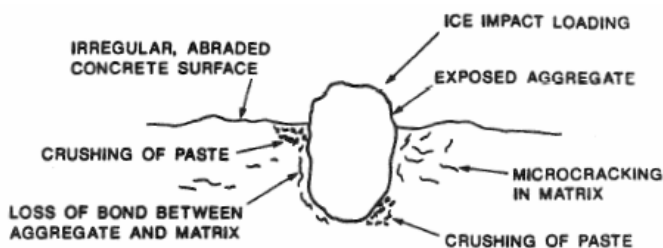


Figure 2.1 Failure mechanism associated with ice floe loading of exposed aggregates

3 DATA

Table 3.1 below summarizes ice abrasion data from various laboratory and field experiments, listing key parameters with emphasis on exposure conditions and concrete material parameters. Ice conditions are also presented for the experiments where these are available.

Table 3.1 – Brief summary of various ice abrasions data from the literature

| Author | Abrasion/ Abrasion rates | Material Parameters | Exposure | Exposure (lab/field) | Comments |
|-----------------------------|--|--|--|--|---|
| Huovinen Field (1990) | 22-39 mm after 22-24 years (mean, all faces) | At water level: fc = 35-46 Mpa 1,5m above WL: fc = 65-80 MPa | Combination of freeze- thaw cycles and moving ice | Lighthouses in the Gulf of Bothnia | Largest abrasion rate observed 0,1-0,3 m below water level |
| Huovinen Field (1990) | 15 mm 3,5 mm 2 mm | LWA, fc = 30 MPa ND1, fc = 50 MPa ND2, fc = 60 Mpa, blast furnace | Specimens mounted at the front of an ice breaker | Ice breaker test, Baltic sea | Assume 40 km ice exposure for all specimens. |
| Huovinen Lab (1990) | > 25 mm 2,5 - 11 mm 3,2 - 7 mm | LWA, fc=41-42 MPa ND1, fc=68-98 MPa ND2, fc=76-81 Mpa, blast furnace slag cement | 50 freeze- thaw cycles and 10 min in abrasion machine | Lab, abrasion machine (rotating cutter) | No ice. |
| Malhotra Field (1996) | No visible abrasion observed after 7 years of exposure. | LWA: fc = 37-45 MPa ND: fc = 42-56 MPa Steel Fibers (SF): 50kg/m ³ w/c ratio: 0,37- 0,42 | “Very severe exposure, included freeze-thaw cycles, ice abrasion, ice impact, and sea water attack.” | 12 panels mounted in a dock at Nanisivik (73° North), Baffin Island, Canada | No description of the ice conditions. Test panels were in good to excellent conditions after 7 years of exposure. Local corrosion of the steel fibres. |
| Malhotra Lab (1996) | Weight loss (%): 1,9-2,4 (LWA) 1,5-1,7 (LWA/SF) 1,1-1,8 (ND) 0,9-1,1 (ND/SF) | Ref.: Malhotra Field (1996) | Tested for 1200 sec (20 min) | 12 specimens tested according to: ASTM C 779 Procedure C | No ice. Use of steel fibres had a positive effect on the abrasion resistance. |

| Author | Abrasion/ Abrasion rates | Material Parameters | Exposure | Exposure (lab/field) | Comments |
|--|---|--|--|--|--|
| Janson Field (1988) | Abrasion depths: 0-140 mm Abrasion rates: 0,2-7,0 mm/year | ND (rounded shape) fc = 40 MPa Cement: 300-400 kg/m ³ Additives: Air-entraining agent (after 1965) | Location in Baltic Sea with low salinity, hence strong ice compared to Arctic seas (first year ice). | Field study of More than 30 light houses examined in 1983-84 | Abrasion depths increased further north (more severe ice conditions). No abrasion in areas where the level ice thickness never exceeded 0.3m |
| Janson Field (1989) | Abrasion rates: 0,3-11,6 mm/year | LWA, fc = 60-70MPa ND, fc = 70-90 MPa | 24 reinforced concrete panels in Baltic Sea 1986-89. Freeze-thaw tests showed good resistance for the panels. | Examination of concrete panels on the most severe light house from the Janson 1988 study. | Most abrasion parallel with ice flow direction. Ice conditions means more to abrasion than the concrete properties. |
| Itoh, Lab (1988, 1994) | Abrasion rate (steady state): 0,05 mm/km for ice parameters given under "exposure" | ND, fc = 57 Mpa LWA, fc = 70, 57, 35 Mpa D _{max} = 25 mm | Ice velocity: 5 cm/sec Ice temp: -20 °C Contact pressure: 1 MPa | Completely exposed aggregates made by cutting the top surface by 6-10 mm | Abrasion rate of concrete due to sea ice is mainly determined by the contact pressure and the ice temperature. |
| Hanada Lab (1996) | Abrasion depth: $S = S_r \cdot \sigma_v \cdot L$ Assume: $S_r = 0.0178$ $\sigma_v = 1 \text{ MPa}$ $L = 1000 \text{ km}$ Abrasion depth: $S =$ 17.8 mm | N.A. | Sea ice: 3-5 ppt salt Ice velocity: 5 cm/sec Ice temp: -10°C Contact pressure: 1 MPa | | Study of ice abrasion rates of different aggregate stones and a single concrete sample. |
| Nawwar and malhotra Lab (1988) | Abrasion depths: Non-textured surface: 0,6-1,1 mm Textured surface: | ND, fc = 35-65 MPa w/c = 0,26 - 0,38 Air content: 5 - 6,5 % | Ice abrasion and/or impact. Impact speed: 1-2,5 m/sec Abrasion speed: | Lab, Ice abrasion machine, rotating, cylindrical specimens | Surface finish of the test specimen greatly affects the initial abrasion resistance of |

| Author | Abrasion/ Abrasion rates | Material Parameters | Exposure | Exposure (lab/field) | Comments |
|-------------------------|---|--|--|---|--|
| | 0,2-0,4 mm Abrasion rates: Non-textured surface: 0,004 mm/km Textured surface: 0,003 mm/km | | 1 m/sec Impact pressure: 6 MPa Temperature for ice- and concrete: -10°C | | concrete. |
| Hara Field (1995) | Max observed abrasion rate: 1.0 – 5.0 mm/year Proposed abrasion rate: $S = 0.0012 \cdot \sigma_v$ where, S = abrasion rate [mm/km] σ_v = ice contact pressure [kgf/cm ²] -10 °C ≥ T ≤ 0 °C | LWC, fc = 57 Mpa | Ice drift typically 20- 30 km/year | Field study of bridge piers in Japan. | Ice abrasion rates largest at waterline. Abrasion rates increases with increasing ice velocity and pressure. Ice abrasion caused exposure of the reinforcement. |
| Sandwell (2003) | Approx. 10 mm estimated by size of exposed coarse aggregates (app.7 years after opening of bridge) | fc = 90 MPa w/c = 0,25 Fly ash + silica fume High Performance Concrete (HPC) Design Lifetime: 100 years | Gulf of St Laurent/ Northumberla nd strait/Canada | Confederati on bridge piers | Based on photos in Sandwell project facilities design report for Sakhalin II, Phase II |
| Fiorio Lab (2005) | Mean abrasion rate: 2 mm/km | fc = 24.8 MPa w/c = 0.6 Portland CEM I 42.5 Aggregate: Fine sand (0.2 – 0.6 mm), coarse sand (3 – 5 mm) | Contact pressure ice/concrete: 0.25 – 0.80 MPa | Lab, Abrasion/ friction tests by a shear- box machine | Laboratory grown S2 columnar freshwater ice (D _{grain} = 8 mm) |

4 LITERATURE REVIEW

4.1 Hoff (1988)

Resistance of Concrete to Ice Abrasion – A Review

In this paper G. C. Hoff presents a review of various publications dealing with the phenomena of ice abrasion on concrete structures. His review does also describe some general abrasion tests, like e.g. studded tire experiments, which does not involve ice. In this summary it is looked into those of the studies which involve abrasion by ice only.

In 1982 a comprehensive three-phase program with emphasize on developing high-strength lightweight concretes for marine arctic structures was launched and included totally five different methods of evaluating the abrasion resistance of concrete. The programs were Phase I, Phase II and Phase III of ABAM Engineers Inc., Developmental Design and Testing of High-Strength Lightweight Concretes for Marine Arctic Structures, Joint Industry Project Report, form now on named; “[ABAM-I]”, “[ABAM-II]” and “[ABAM-III]”, respectively.

In the first phase of the study “[ABAM-I]”, a test apparatus was developed and tested under various conditions. The test configuration consisted of several concrete discs with different mixtures mounted on a horizontal shaft. The discs were rotated at velocities between 100-500 rpm. Stationary ice blocks were pressed against the rotating concrete specimen with compression stresses of 2.1 - 3.4 MPa. As the test method did not take any precautions against the so called ad freeze effect, ice immediately started to grow on the concrete surface and therefore preventing the ice to have any abrading effect on the concrete. Neither changing the speed of rotation, nor varying the ice pressure or the temperature did solve this problem. The test was therefore terminated without achieving any data on ice abrasion. As this test program started back in 1982 it was clearly in the early childhood of laboratory testing of ice abrasion. The majority of the tests presented in this overview were executed in the late eighties or mid nineties.

In the next study “[ABAM-II]”, concretes were evaluated for abrasion resistance both by a team in the USA and a team in Japan. Two similar tests in each of the countries were done in parallel on specimens from the same concrete batch. The first test was the so called ASTM Method C779, “Abrasion Resistant of Horizontal Concrete Surfaces, Procedure A (Revolving discs)” which is a mechanical test and does not include ice. The results from the US showed that lightweight aggregate concretes (LWAC) performed better than the reference normal weight concrete (NWC). The Japanese results from the same test showed the opposite relation between LWAC and NWC, i.e. that the NWC showed the best abrasion resistance. No evaluation of the discrepancy was made in the study.

The second test in the US was a tumbler abrasion test. The machine had a variable speed belt drive which was set for its lowest operating speed at approximately 10 rpm for the abrasion testing. The test specimens were concrete slabs (241 x 267 x 51 mm) of the same 4 batches as for the previous ASTM Method C779 test. Some of the concrete surfaces were made smooth while others were rough in order to study the effect of the roughness with respect the abrasion properties. All specimens received 14 days moist curing followed by 14 days of air drying before testing. The test arrangement is shown in Fig 4.1. Nineteen slabs were tested at the same time. The abrasive material at the first 5 weeks of the test was only freshwater ice. Wear measurements after the 5 weeks showed no significant wear regardless of the type of surface finish. After the 5 week period and for the following 19 weeks, the abrasive material was changed from freshwater ice to coarse aggregates, ice and grit, where the ice had the purpose of being a carrier for the grit.

The results of the latter 19 weeks are shown in Fig 4.2 and 4.3. All the specimens seemed to have a higher wear rate for the first couple of weeks, and then it remained fairly constant for the next few weeks, followed by an increase at a relatively uniform rate for the rest of the test. All the lightweight aggregate concretes experienced more abrasion than the normal weight aggregate concrete. The effect of the surface texture was only traceable for the first couple of weeks of the test (i.e. the first few weeks after the coarse aggregates and the grit were introduced as an abrasive medium). The smooth surface abraded less than the rough surface for the weeks in question.

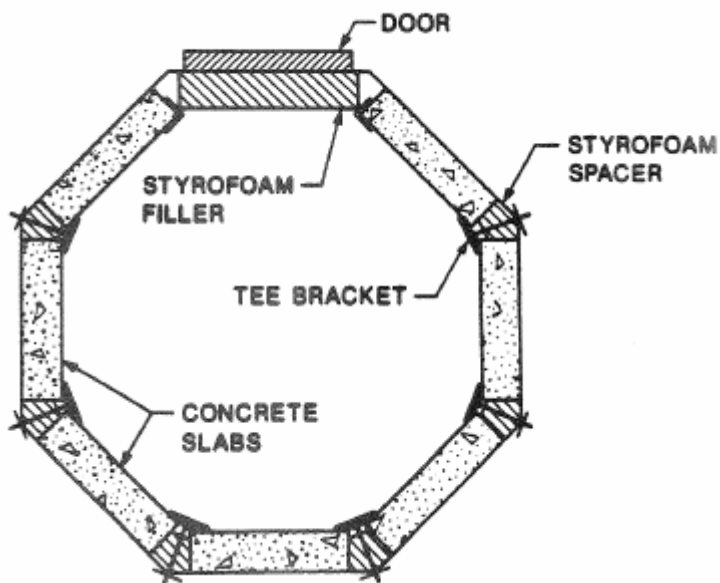


Figure 4.1 Cross section of the tumbler barrel showing specimen arrangement [12]

Table 4.1 – Compressive strength for the specimens in the tumbler abrasion test

| Label | Material | f_c [MPa] |
|-------|------------------------------------|-------------|
| NWC | Normalweigh concrete | 48 |
| LWC1 | Lightweight concrete | 48 |
| LWC2 | Lightweight concrete | 48 |
| HSLWC | High strength lightweight concrete | 62 |

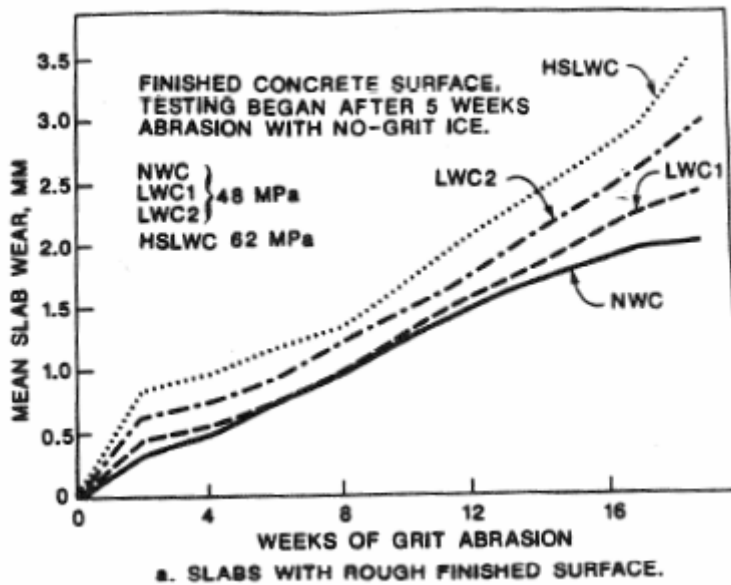


Figure 4.2 Mean abrasion versus exposure time [weeks] for slabs with rough surface [12]

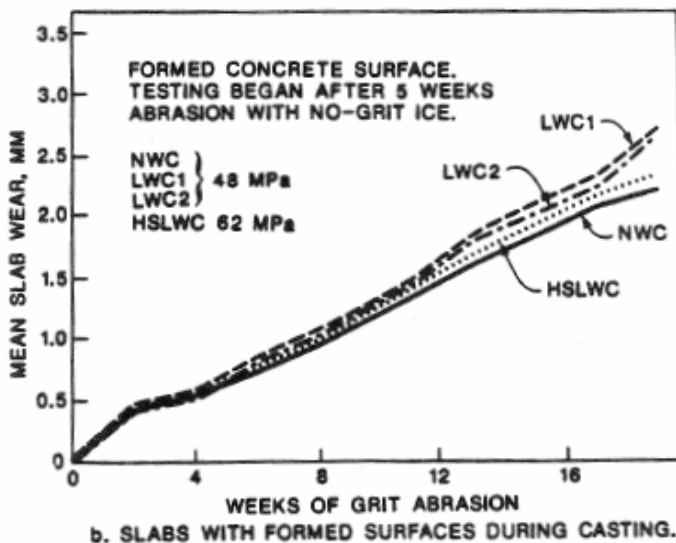


Fig. 9--Effect of surface finish and concrete types on tumbler abrasion test results (11)

Figure 4.3 Mean wear versus exposure time [weeks] for slabs with smooth surface [12]

The second test in Japan involved an ice abrasion machine with a revolving disc as shown in Fig 4.4. The machine was located in a room with constant air temperature of $-20\text{ }^{\circ}\text{C}$. The specimens were reinforced, hollow LWAC and NWC concrete cylinders with diameters 300/190 mm (outer/inner, respectively) and a height of 100 mm. All specimens were moist cured in 14 days after casting followed by an air drying period varying from 29-39 days at $+21\text{ }^{\circ}\text{C}$ and 50% relative humidity. The saline ice blocks used in the test were shaped into pieces of 400 mm in diameter and 120 mm high. The ice cylinders were laterally supported by a thin steel plate in order to preserve their shape during testing. The test was activated by gradually lowering the ice blocks onto the rotating concrete specimens. Pressure levels varied between 0.5 and 1.0 MPa.

The revolution speed was 60 rpm corresponding to an ice velocity of 2.78 km/h. It was necessary to manually replace the ice block every hour during the test. The problem with ad freeze (build-up ice) on the concrete surface was solved by applying ethanol at each ice block replacement. At the same time any concrete debris etc was also removed from the interface between concrete and ice. Each test had a run of approximately 16 hours a day, including the necessary stop periods due to abrasion measurements and replacements of the ice blocks, and continued for 5 days running for each specimen corresponding to a total ice contact length of 180 km. The abrasion was measured by both an electrical dial gage and manually using a template and a standard dial gage. The test results are shown in Fig 4.5 – 4.7. The effect of the ice contact pressure is a very important parameter, especially for large contact lengths. At contact pressure 0.5 MPa, the coarse aggregates were hardly exposed during the entire test period. For a contact pressure of 1.0 MPa however the lightweight aggregate concrete showed a relatively large wear compared to the normal weight aggregate concretes.

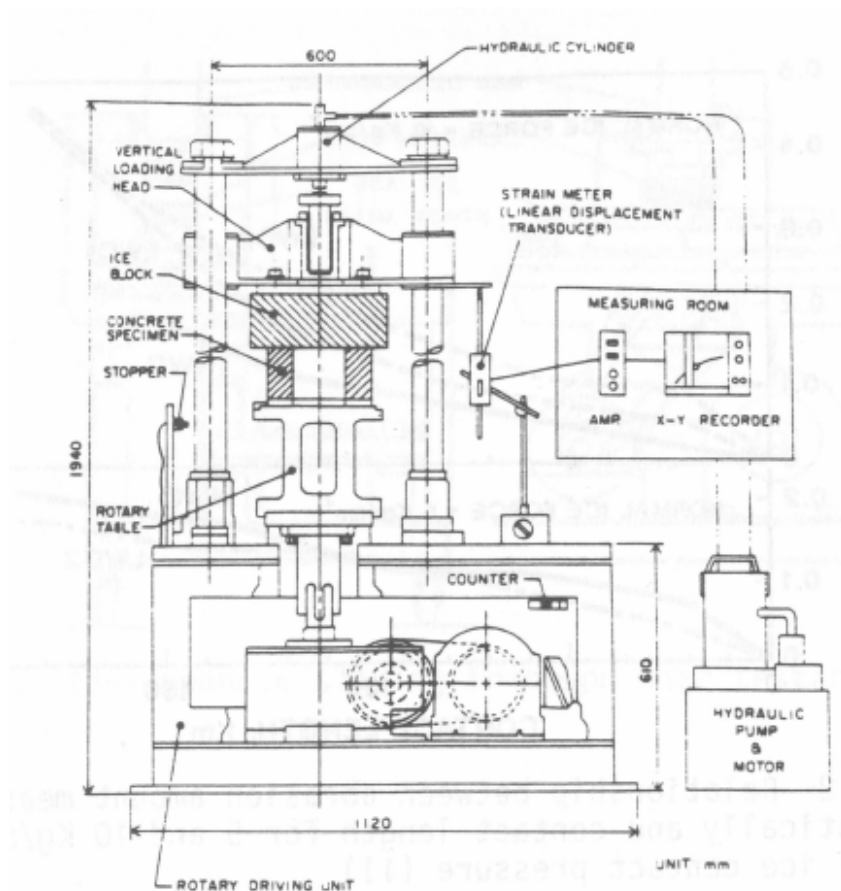


Figure 4.4 Principle sketch of ice abrasion apparatus with the revolving disc concept [12]

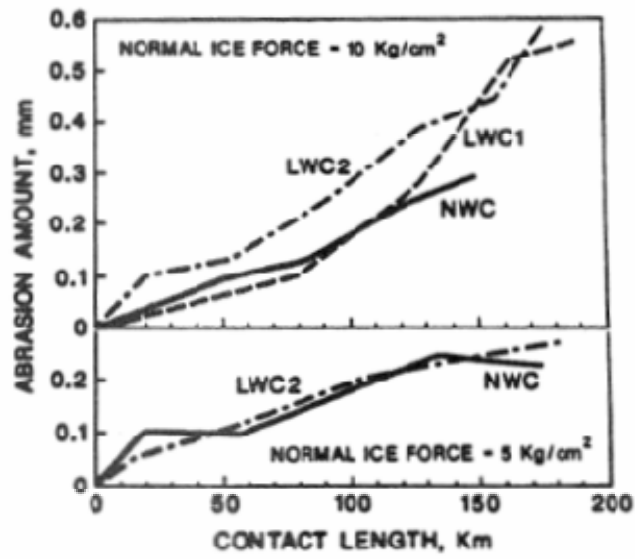


Figure 4.5 Mean abrasion versus ice contact length [12]

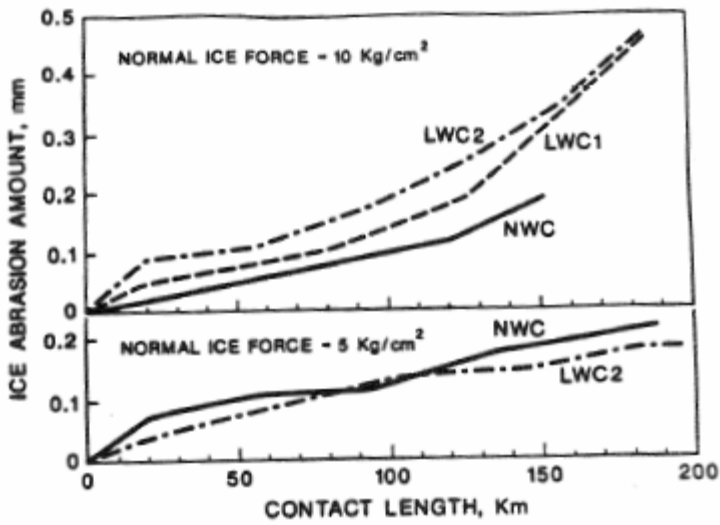


Figure 4.6 Mean abrasion versus ice contact length [12]

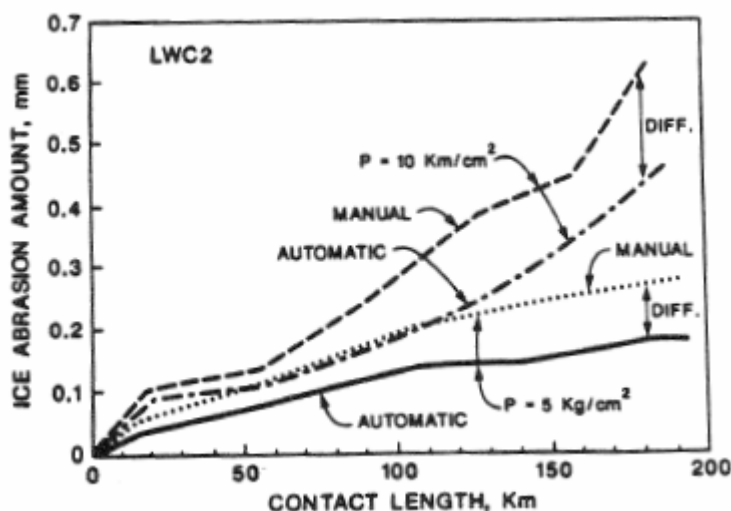


Figure 4.7 Mean abrasion versus ice contact length [12]

In the third and last study “[ABAM-III]”, concretes were tested against sea ice abrasion in a sliding friction apparatus as shown in Fig 4.8. A stationary concrete specimen, formed as a frustum of a pyramid, had its smaller base pressed down at the sliding ice block below. Concrete aggregates included in the test were;

- a) High-strength concrete with ordinary aggregates
- b) High-strength lightweight concrete with lightweight coarse aggregates and ordinary fine aggregates
- c) High-strength lightweight concrete with both lightweight coarse and fine aggregates.
- d) One of the concrete specimens had a Zebron (low friction coating) coated surface.

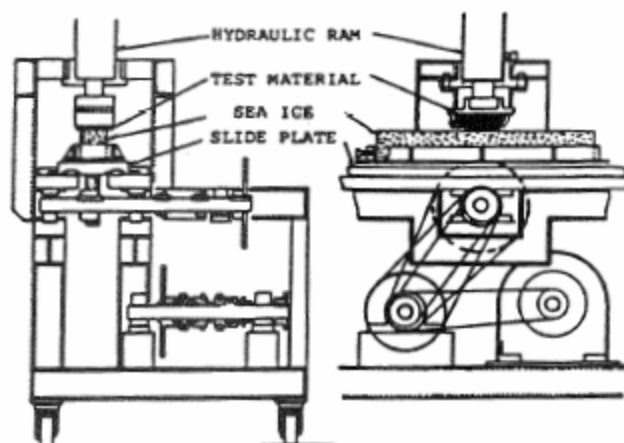


Figure 4.8 Principle sketch of sliding friction apparatus [12]

All 3 concretes had a 28 days compressive strength of 56 MPa. The sea ice block was 80 mm wide, 50 to 100 mm high and 700 mm long and was placed inside a steel box. Fresh water was filled in between the ice block and the steel box, i.e. along the ice block periphery, and allowed to freeze in order to secure the lateral support of the ice during the test period. Each stroke of the reciprocation movement was 500 mm and the speed was varied between 20, 50 and 200 mm/sec. The study also examined potential effects on ice abrasion originating from the anisotropic nature of sea ice, i.e. a simulation of ice moving along a sloped concrete surface.

All tests were performed with a temperature of -20°C with an ice pressure of 1 MPa and an ice speed of 50 mm/sec. Air was blown at the surface of the specimens to remove the small abraded ice and melt water. After each of the tests the abrasion depths of the concrete were measured along five evenly distributed lines across the surface of the specimen. The abrasion representation of each specimen was obtained by averaging the measured depths from these five lines.

Sea ice is a crystalline material and its properties depend heavily on the size and orientation of its crystals. Parameters such as e.g. temperature, salinity and density have all important roles to play in the process of forming sea ice. In Fig 4.9 the effect of the ice grain orientation with respect to abrasion is studied. The data named "Type A" in the test series is when the sea ice is loading a sloped surface and "Type B" when the sea ice is loading a vertical surface. As seen, the results indicate that the brine orientation of the sea ice does not significantly influence on the abrasion.

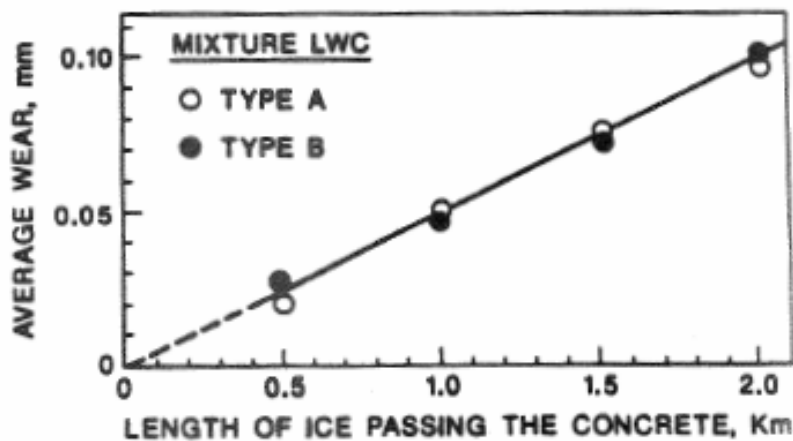


Figure 4.9 Effect of ice grain orientation versus mean abrasion [12]

In Fig 4.10 the abrasion rate with respect to sliding distance is plotted. As seen, there is no evident divergence between the different types of aggregates with respect to the wear rate. After an initial stage, say up to approximately a contact length of 7 km, the abrasion seems to reach a constant rate with a mean wear rate of approximately 0.05 mm/km (0.1 mm/2km).

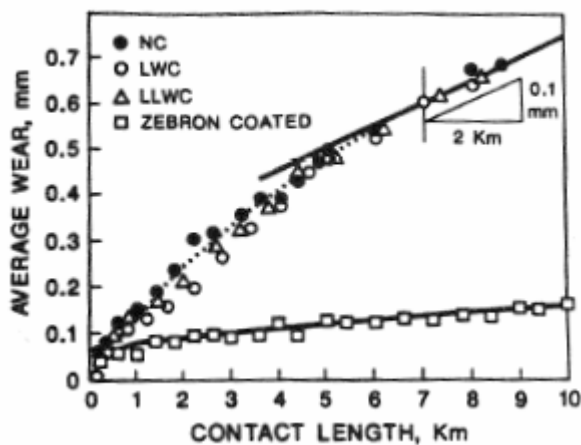


Figure 4.10 Mean abrasion versus ice sliding distance [12]

In order to study the phase of abrasion when the coarse aggregates were fully exposed, the outermost 10 mm of the specimen's surface were sawn off. The results from these tests are presented in fig 4.11 showing a constant abrasion rate. As in the results discussed above, initial high abrasion is due to abrasion of the surface paste layer, whereas steady state abrasion of the bulk concrete including paste and aggregate is reached. The numerical value of the abrasion constant does also correlate well with that of the test results in Fig 4.10 and 4.11, i.e. a mean wear rate of approximately 0.05 mm/km.

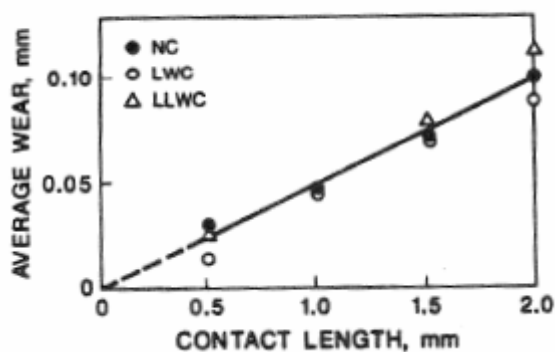


Figure 4.11 Mean abrasion vs. ice sliding distance for specimens with exposed aggregates [12]

Fig 4.12 shows the average wear of the concrete surface as a function of the contact pressure between ice and concrete. All the specimens were tested for an ice contact length of 1.0 km for the given stresses. The test suggests that the abrasion rate is proportional to the contact pressure.

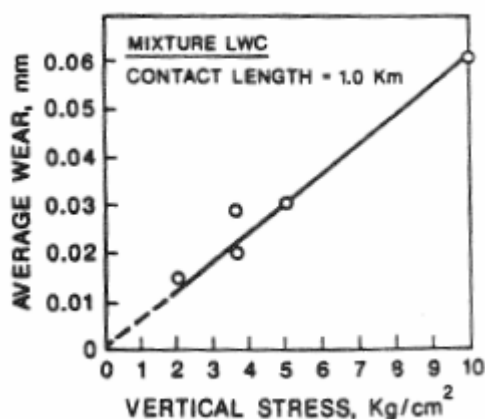


Figure 4.12 Average wear as a function of ice contact pressure [12]

Finally, Fig 4.13 shows the ice temperature's influence on the average abrasion rate. The results indicate that for ice temperatures above (warmer than) -10°C , there is no observable difference between the various aggregates with respect to the wear rate. It is also observed that wear rate itself holds an almost constant value for temperatures above -10°C . For ice temperatures below -10°C , it seems to be a distinct change in the average abrasion rates, especially for the concretes with normal weight aggregates (NC) and the lightweight concretes with coarse aggregates and ordinary fine aggregates (LWC).

It is somewhat surprising that the concrete with the lightweight coarse and fine aggregates (LLWC) shows an average wear rate that is only half of the NC and LWC at a temperature of -20 °C. The mean abrasion rate of LLWC is in fact at the same order of magnitude as the low friction coating. This is interesting findings and should be subject to further studies.

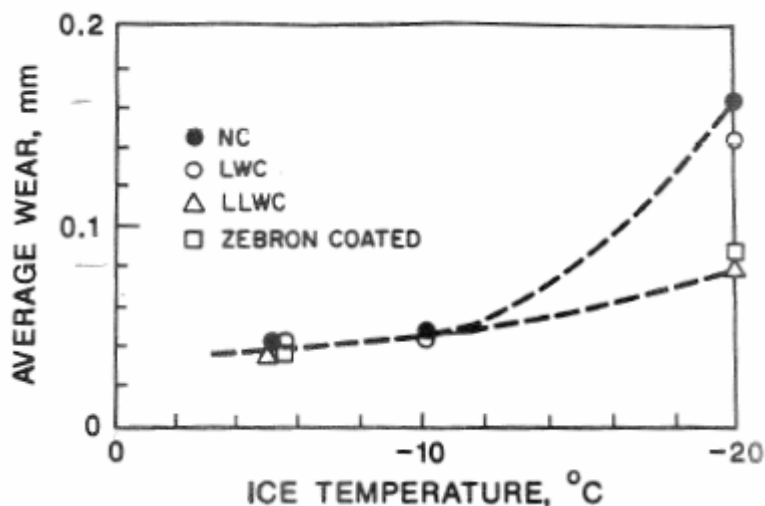


Figure 4.13 Ice temperature's influence on the average abrasion rate [12]

To sum up the ABAM investigations reported by Hoff, ice abrasion rates seemed to be higher in the initial stages with paste on the surface. Abrasion increased with increasing ice pressure and decreasing ice temperatures, whereas the effect of material quality is more uncertain, as little information is given about w/c ratios, compressive strength, additives, cement replacements, air content, etc.

4.2 Nawwar and Malhotra (1988)

Development of a Test Method to Determine the Resistance of Concrete to Ice Abrasion and/or Impact

This study describes the design and development of a test apparatus for determination of the resistance of concrete to ice abrasion and/or impact. In the study concrete cylinders with diameter 300 mm and length 500 mm are used. The ice contact pressure is obtained by an ice block with a temperature of -10 °C located above the rotating concrete specimens (cylinders) below. For the abrasion tests the speed of the rotating specimens were set to 1 m/sec. In order to avoid ice growth on the surface of the concrete cylinders during testing, the specimens were approximately one third submerged in water with a salt content of about 30 parts per thousand (ppt) and with temperatures between 1 and 5 °C. As a consequence of this wet testing arrangement, the concrete surface was significantly warmer than -10 °C and thereby also the ice block which lead to a higher consumption rate of the ice. The ice in use was laboratory grown saline ice with salinity in the range of 3 to 5 ppt, which is close to naturally occurring first year sea ice. The test was performed continuously for periods of 6-8 h, which corresponds to the duration of wear of each ice block. As each block wore out, the test was stopped until a new block was in place. When examining the test results it was found that the specimens mounted on the "left" side of the test machine sustained more wear than the one mounted on the "right" side. As both the concrete test cylinders rotate in the same direction, this was believed to induce different loads to the specimens and hence be the cause of this deviation.

The variation was believed to be eliminated by counter rotating the specimens and the authors therefore suggested such a modification under their conclusions. During impact testing, strain gauge responses were measured and recorded from gauges mounted on the reinforcement bars inside the concrete specimens. The authors stated that no conclusive results could be obtained from these gauges as their response varied erratically under increasing forces. Hence, the impact testing is therefore not discussed any further in this summary of the study.

The authors emphasize the importance of taking the following aspects into consideration when designing equipment for use in abrasion testing:

- In order to get reliable results from the abrasion testing, the need of having a sufficiently large surface area of the test specimens is underlined.
- One should aim at creating exposure conditions as realistic as possible compared to the actual field conditions.
- Keep the mechanical complexity of the equipment at a minimum and use a micro computer for automatic control.

Based on the criteria above, the following parameters were chosen for the test:

- Abrasion speed: 1 - 2.5 m/sec
- Size of concrete specimens/cylinders: diameter: 300 mm, length: 500 mm
- Impact stress and area: Impact area: 0.03 m^2 , Impact stress: 6 MPa
- Ice blocks: height: 300 mm, length: 800 mm, width: 350 mm
- Ice properties: salinity: 3-5 ppt
- Temperature: Air and ice temperature: $-10 \text{ }^\circ\text{C}$

The following conclusions were made from the test results:

- Dry abrasion conditions lead to growth of an ice layer on the concrete test cylinders which work as a protective layer with respect to abrasion.
- Wet abrasion conditions indicate that the ice abrasion rate varies as a function of local contact pressure between ice and concrete, surface finish (roughness), and the strength of the concrete.
- The wear (abrasion) rate is highest in the beginning of the test, whereas it after a while drops to something that seems to be a steady state rate. The surface finish of the concrete specimens affects the initial abrasion rate.
- The local ice pressure on the concrete surface significantly affects the wear. A reduction in the surface pressure reduces the abrasion considerable.
- Mean abrasion rate: Non-textured surface: $0,0003\text{-}0,003 \text{ mm/h} = 0,004 \text{ mm/km}$
- Mean abrasion rate: Textured surface: $0,0004\text{-}0,005 \text{ mm/h} = 0,003 \text{ mm/km}$
- At least three sets of cylinders, with each set consisting of two cylinders, should be tested to obtain meaningful data for any given test condition.
- Mean annual abrasion rate interval: 0.43 to 0.65 mm/year, given 3 months of active ice actions for 10 percent of the time. The wear rate will be proportional to the duration of the ice activity.

The authors list the following recommendations with respect to improvements of equipment and further studies:

- Modifications to the apparatus should be done in order to eliminate unequal loading on the two test cylinders.
- Testing of various concrete qualities with different surface finishes should be carried out in order to develop statistical data from which abrasion limits could be established.
- Grit (sand) embedded in ice is an observed phenomenon and its effect on ice abrasion rates on concrete should be closer investigated.

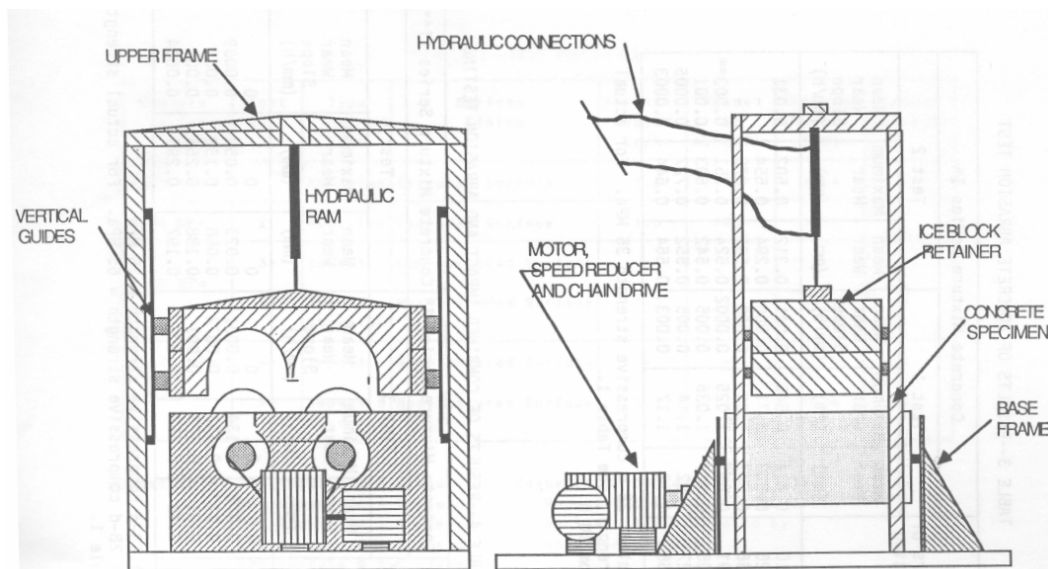


Figure 4.14 – Ice impact/abrasion test apparatus, Principle sketch [11]

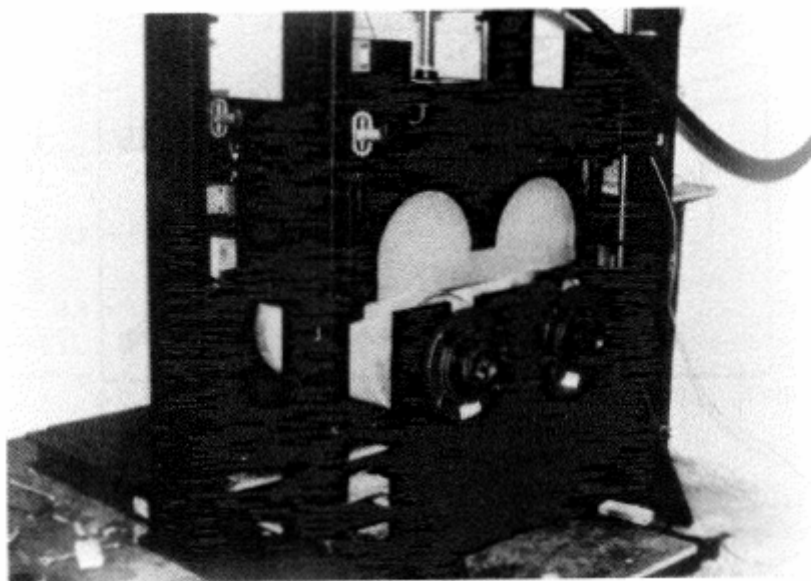


Figure 4.15 – Ice impact/abrasion test apparatus [11]

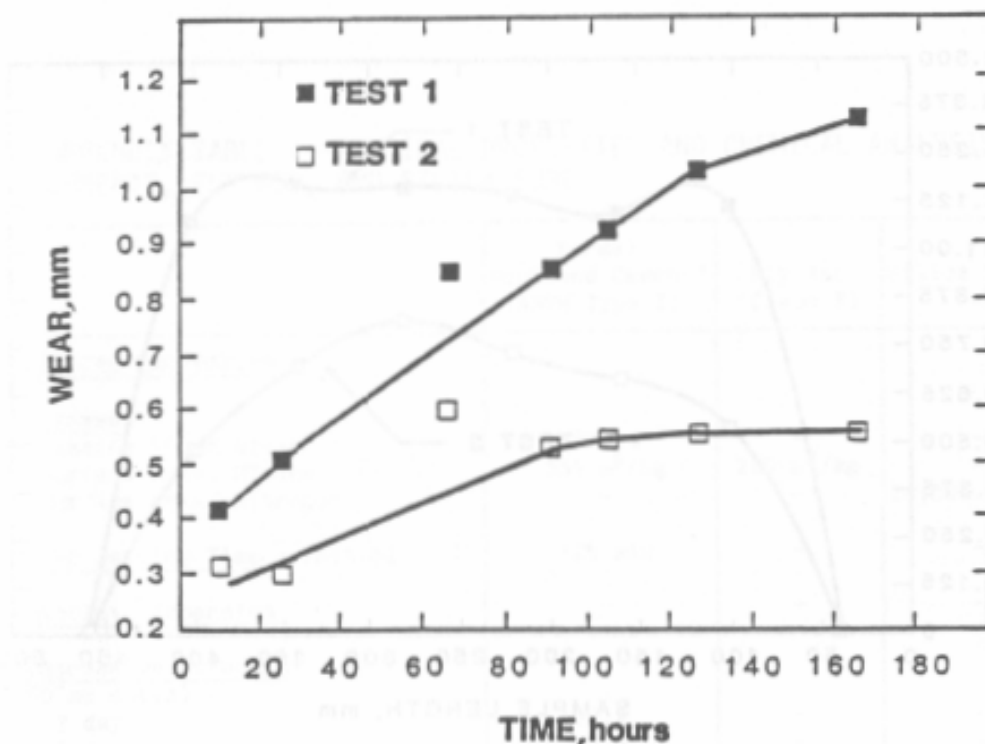


Figure 4.16 – Ice abrasion test – mean wear vs. time for Test 1 and 2 (non-textured surface) [11]

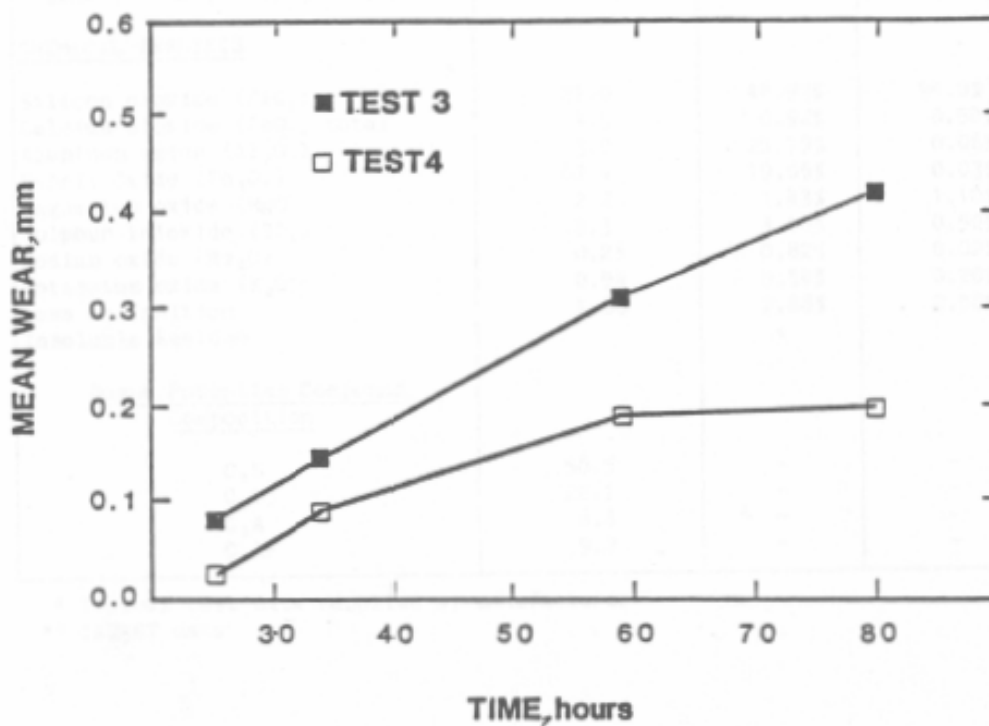


Figure 4.17 – Ice impact and abrasion test – mean wear versus time for Test 1 and 2 (textured surface) [11]

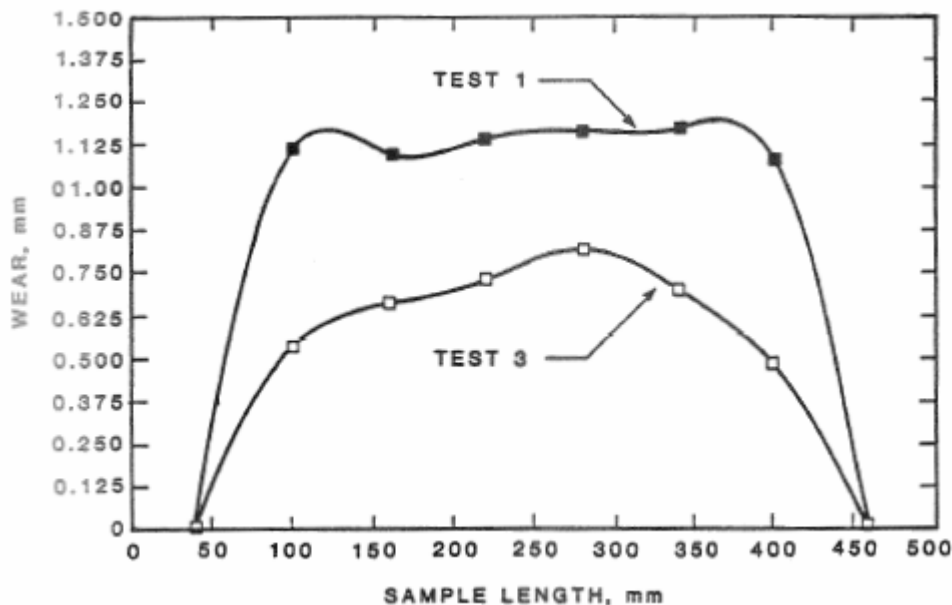


Figure 4.18 – Surface profiles of concrete cylinders – mean wear versus specimen length [11]

4.3 Itoh et al. (1988 & 94)

An Experimental Study on Abrasion of Concrete Due to Sea Ice/ Estimation Method for Abrasion of Concrete Structures Due to Sea Ice Movement

In this study it is suggested an estimation method for determination of the ice abrasion of concrete structures due to ice movement. The investigations are based on laboratory tests of various types of concrete. There is unfortunately not shown any principle drawing over test apparatus, and the written description of the actual test procedure is also poor. The description of the laboratory test reads as follows: “The device used for abrasion testing has an abrasion mechanism of the alternating motion type.” In order to examine the adequacy of the proposed estimation method, there have been made a comparison with the results of Janson lighthouses [14, 15].

Six different types of concrete are subjected to the abrasion test;

NC: Normal concrete of compressive strength $\sigma_c = 57$ MPa (568 kgf/cm²) containing ordinary coarse and fine normal weight aggregates

LWC: High-strength lightweight concrete of $\sigma_c = 70, 57, 35$ MPa (700, 568, 350 kgf/cm²) containing ordinary fine and lightweight coarse aggregates

LLWC: High-strength lightweight concretes of $\sigma_c = 57$ MPa (568 kgf/cm²) mixed with lightweight coarse and fine aggregates

A concrete specimen protected by a layer of 500 μ m Zebtron low friction coating.

In Fig 4.19 the relationship between the mean abrasion and the sliding distance is shown. In the figure there are referred to 3 different regions, of whom each indicating different stages in the abrasion process.

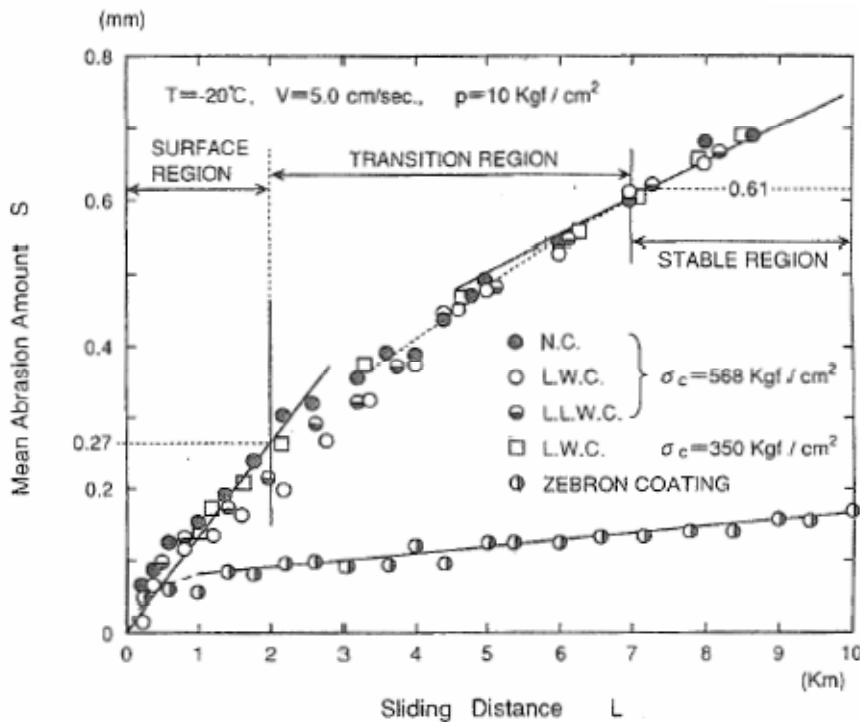


Figure 4.19 Change of mean abrasion amount with sliding distance [14, 15]

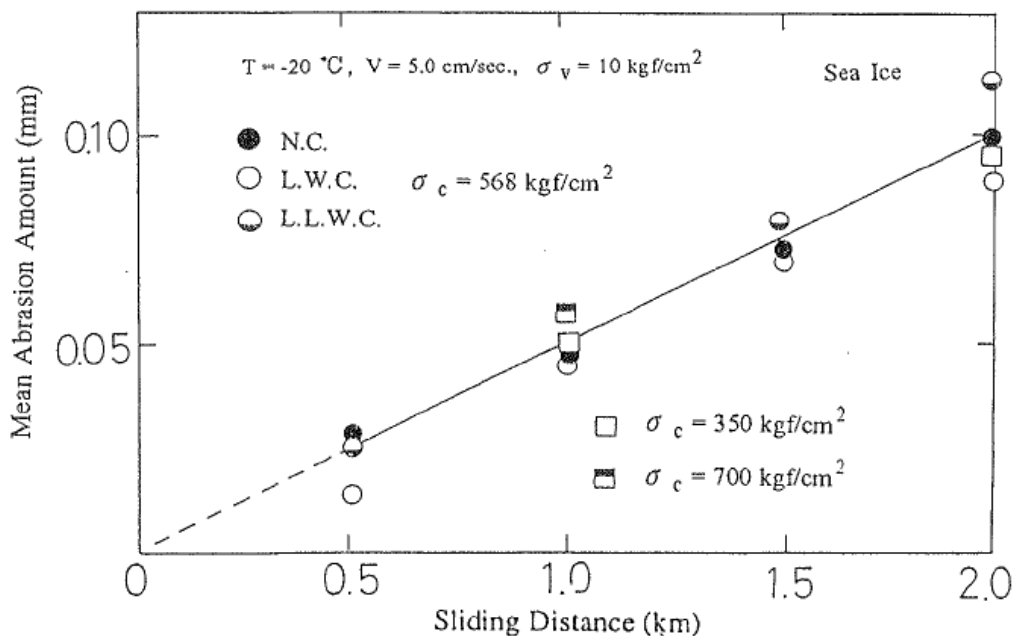


Figure 4.20 Mean abrasion versus sliding distance, outermost 10 mm of surface sawn off [14, 15]

As seen from Fig 4.20 the relationship between the mean abrasion and the sliding distance approximates a straight line already from the start when the outermost 10 mm of the concrete surface is sawn off, and the mean abrasion rate reads 0.05 mm/km. It is also observed that the mean abrasion rate is constant for the different concrete qualities, regardless of compressive strength and type of aggregates. The authors used this “accelerated method” to shorten the test time considerably for the remaining experiments. From an engineering point of view it is also the steady state abrasion rate that is the main target and the most interesting one.

From Fig 4.19 it is seen that both the “surface region” abrasion rate and the “transition region” abrasion rate are valid for sliding distances below 7 km under the given test conditions. That short sliding distances are not considered of any practical interest when it comes to design of e.g. arctic sea structures exposed to thousands of kilometres of ice drift during their life time. Hence the accelerated test contributes to a more rational test procedure and a simpler relation between abrasion rate and ice sliding distance.

The test conditions were as follows;

Ice sliding velocity, $v = 5.0$ cm/s

Ice temperature, $T = -20^{\circ}\text{C}$

Contact pressure, $p = 1$ MPa (10 kgf/cm²)

With the given test conditions it seems that the abrasion rate depends neither on the compressive strength of the concrete nor the kind of concrete aggregate.

It was suggested that the abrasion rate of concrete is mainly determined by ice temperature and contact pressure. Considering the lack of data on the concrete it is not possible to determine the relative importance of varying exposure- and material parameters. The effect of the ice temperature and the contact pressure is illustrated in Fig 4.21 and 4.22, respectively.

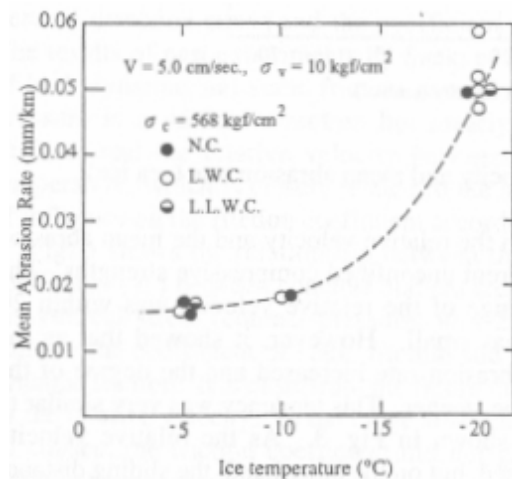


Figure 4.21 Abrasion rate vs. ice temperature [14, 15]

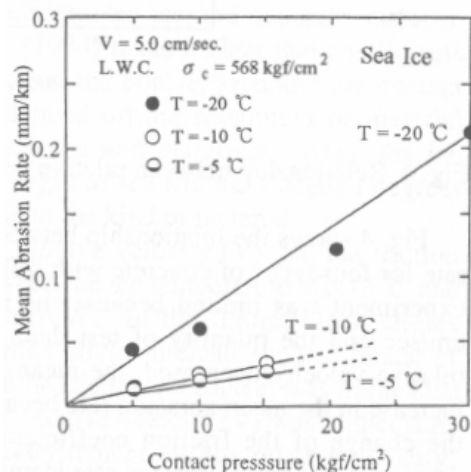


Figure 4.22 Abrasion rate vs. contact pressure, [14, 15]

Using the combination of contact pressure and ice temperature, an empirical formula for the abrasion rate is suggested:

$$S_r = p(9.708T^2 + 1295.7) \cdot 10^{-6} \quad , \quad (\text{Eq 4-1})$$

where S_r - rate of abrasion [mm/km]
 p - ice contact pressure [kgf/cm²]
 T - ice temperature [°C]

Abrasion design curves obtained from this formula is expressed in Fig 4.23.

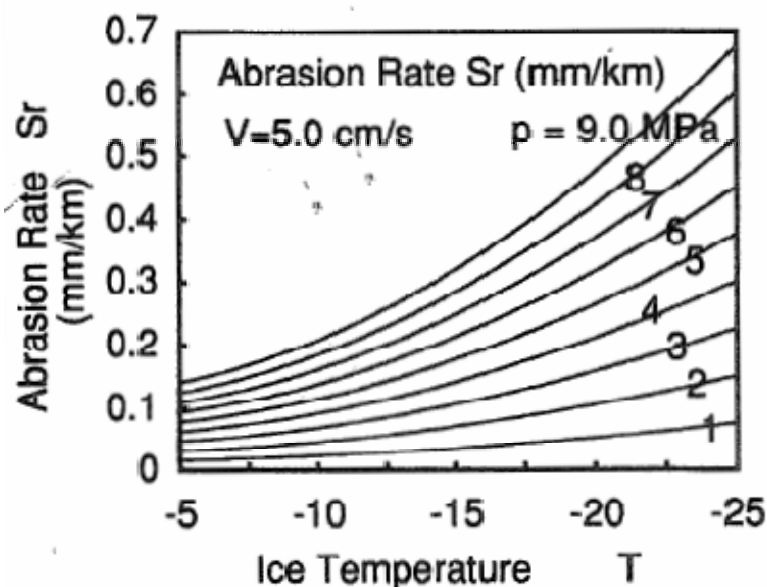


Figure 4.23 Concrete abrasion design curves due to sea ice movement [14, 15]

The effect of ice containing fine sand was also investigated, and this gives an even higher abrasion rate. Both increasing amount and increasing particle size of the fine sand increased the rate of abrasion.

As a check, the proposed formula Eq. 4-1 for estimation of abrasion rate can be compared with the results of the field investigations on the Sydostbrotten lighthouse in the Gulf of Bothnia. Assuming the ice contact pressure to be 4.5 times the uni-axial compressive strength of the ice (based on previous studies) the abrasion calculated by using the formula coincides relatively well with the observed abrasion at the lighthouse. Hence the formula is verified to give reasonable results of concrete abrasion due to sea ice movement.

The study concluded that failure modes of ice sheets are crushing with radial cracking. The abrasion depth of the concrete is mainly governed by the ice parameters; contact pressure, temperature, and sliding velocity.

As the study lacks an overview of the concrete material parameters the conclusions cannot be evaluated with respect to potential material effects on the wear rate. For this purpose; further studies with emphasize on the material properties are needed in order to clarify its role on the abrasion resistance.

4.4 Hanada et al. (1996)

Abrasion Rate of Various Materials Due to the Movement of Ice Sheets

In this laboratory experiment Hanada et al. studied the ice abrasion rates of different aggregate stones (i.e. different types of rock) and a concrete sample in a sliding test apparatus as shown in Fig 4.24 below. The ice abrasion machine was originally developed by Saeki et al (1985) and has the following features; hydraulic controlled surface contact pressure, alternation possibilities between static and kinetic friction, blowing of shaven ice (by an air compressor) and restraining of the generation of frictional heat. The test conditions were as follows;

| | |
|---------------------------|----------------------------------|
| Ice sliding velocity | $v = 5.0 \text{ cm/s}$ |
| Ice temperature | $T = -10 \text{ }^\circ\text{C}$ |
| Contact pressure | $p = 1 \text{ MPa}$ |
| Sea ice with salt content | 3-5 ppt |

The authors state that the above mentioned test conditions were selected according to the following knowledge from results obtained in previous experimental studies:

- Sea ice temperature does not drop below $-10 \text{ }^\circ\text{C}$ due to heating by underlying sea water and insulation by snow accumulation on top of the ice.
- Ice temperatures hardly effects the abrasion rates if above (warmer than) -10°C .
- Ice abrasion rates are proportional to the ice contact pressure.
- The relative ice sliding velocity does hardly affect the abrasion rates.

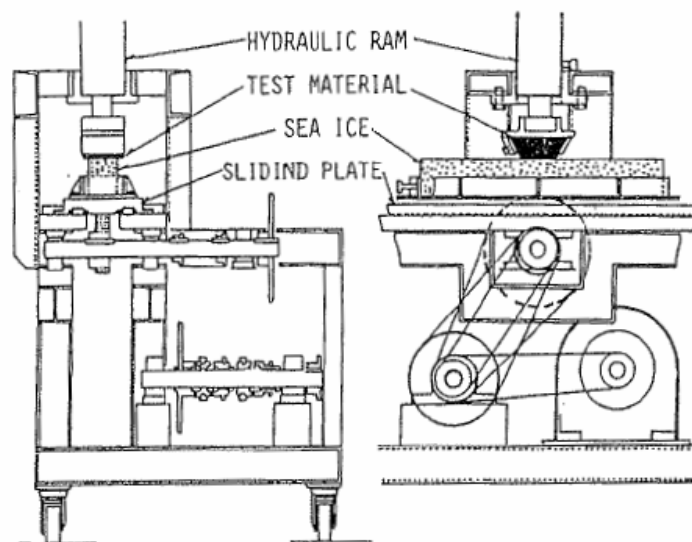


Figure 4.24 Ice abrasion test apparatus (Saeki et al. 1985) [17]

Fig 4.25 shows the average abrasion rate of concrete and various types of stones as a function of ice sliding distance. From Fig 4.25 it seems that the dashed line for the concrete is based on a previous study as there are no signs of curve fittings to experimental data as for the stones (ref legends in upper left corner of the figure). Hanada et al [17] refer to previous studies where it is shown that there exists a relationship between the ice sliding distance and the abrasion amount of concrete that can be divided into three regions depending on the accumulated amount of abrasion; surface region, transition region and stable region (steady state). In order to eliminate the start up effects of the concrete abrasion test, they decided to cut off 1 cm from the surface and thereby presumably jump directly into the stable region.

For the rock samples, however, no effects of the initial unevenness of the surface were observed which proves that the amount of ice abrasion of stone is directly proportional to the ice sliding distance (no transient start up effects). As seen in Fig 4.25, both Sandstone and Andesite show better abrasion resistance than the concrete. Unfortunately, no concrete material parameters such as e.g. compressive strength and w/c ratio are given, so from a concrete technology point of view it is difficult to comment on the abrasion rates between the concrete and the stones. The authors refer to previous studies that indicate that the ice abrasion rates of concrete do not depend upon the uniaxial compressive strength, or the aggregates.

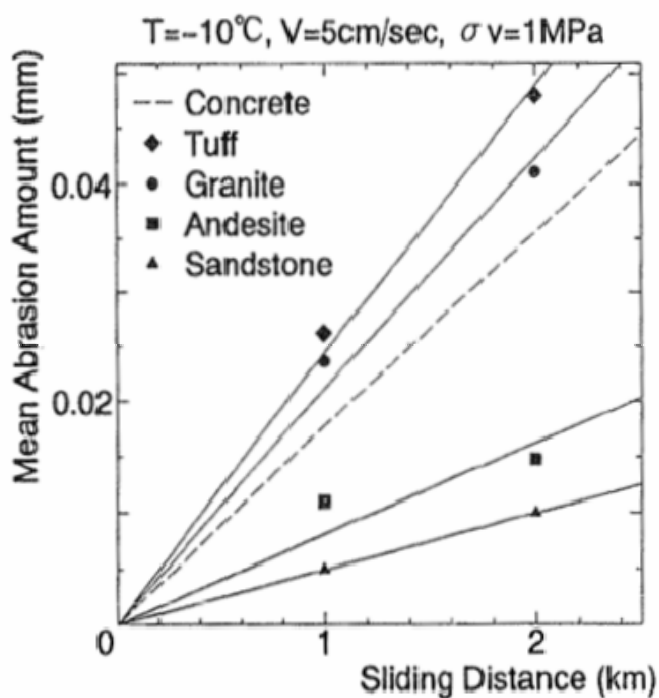


Figure 4.25 Ice abrasion rates for concrete and various aggregates (stones) vs ice sliding distance [17]

Table 4.2 below summarizes the experimental results obtained from [17]. It is noted that the abrasion rate for the sandstone lies below 1/3 of that of concrete. On the other side, both granite and tuff are found to abrade more than concrete (approximately 20 to 40% more, respectively).

Table 4.2 Ice abrasion rates of various materials measured in the apparatus shown in figure 4.24 [17]

| T= -10°C, σ_v = 1MPa | |
|-----------------------------|--------------------------|
| materials | abrasion rate (mm/km) |
| | sea ice |
| concrete | 0.0178 |
| steel | 0.0030 |
| polyurethene | 0.0030 |
| zebron | 0.0078 |
| LDPE | 0.0022 |
| sandstone | 0.0049 |
| tuff | 0.0251 |
| pyroxene andesite | 0.0084 |
| dacite A | 0.0065 |
| dacite B | 0.0177 |
| granite | 0.0216 |

As shown in Fig 4.26 below it seems to be a relation between the ice abrasion rate and the (uniaxial) compressive strength of the rock, as the abrasion rates tend to decrease with increasing compressive strength. According to the authors, only a small number of specimens are tested so that should be borne in mind when considering the reliability of the results. However, the results do at least indicate a relation between the two parameters as stated above. Furthermore, it was observed that the surfaces of sandstone and andesite, most of whose grain diameters are small, showed smooth surfaces after the abrasion tests. On the opposite side of the scale significant surface roughness were observed on the tuff and granite stones. Compared with the abrasion results it is clear that the abrasion rate also seems to depend on the grain size. Surfaces with large grains are rough which leads to an increased friction coefficient and therefore an increased frictional stress and also a higher abrasion rate.

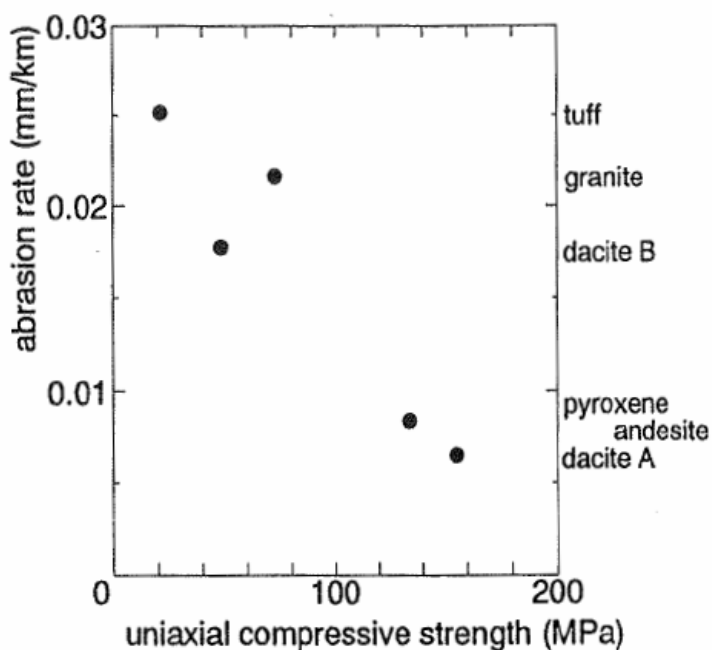


Figure 4.26 Ice abrasion rates of various types of rock vs. (uniaxial) compressive strength [17]

The authors refer to a previous study by Itoh et al. (1994) with respect to which parameters to include in an equation for estimation of the ice abrasion rate. Itoh et al. (1994) concluded that the ice contact pressure and the sliding distance of the ice are the two main parameters to take into account when estimating the average amount of ice abrasion. Based on this, Hanada et al. (1996) suggests the following expression for the total average ice abrasion depth of a given material:

$$\text{Abrasion depth: } S = S_r \cdot \sigma_v \cdot L \quad (\text{Eq. 4-2})$$

where:

- S : Total average abrasion depth [mm]
- S_r : Abrasion rate for the exposed material [mm/km/MPa]
- σ_v : Contact pressure between ice and structure [MPa]
- L : Total sliding distance of the ice [km]

As an example of use of Eq. 4-2 let us assume the following:

From Table 4.2 we have $S_r = 0.0178$ for concrete. If a contact pressure of $\sigma_v = 1$ MPa assumed, and a total ice sliding distance of 1000 km, the following estimated total average abrasion depth can be calculated:

$$\text{Abrasion depth: } S = 0.0178 \cdot 1.0 \cdot 1000 = 17.8 \text{ mm}$$

The conclusions of this study (Hanada et al. (1996)) are summarized as follows:

- The observed ice abrasion rates of rock are proportional to the sliding distance of the ice.
- The abrasion rate differs significant depending on the type of rock
- Abrasion rates of sandstone and andesite are approximately 1/3 of that of concrete.
- The smaller the grain size, the smaller the abrasion rate (related to surface roughness).
- The higher uniaxial the compression strength of a rock, the higher the ice abrasion resistance.

The ice abrasion apparatus in figure 4.24 seems to perform well, showing reduced ice abrasion with increasing strength over a wide range of strengths ($\approx 30 - 160$ MPa). Test details, for example on how to avoid so-called adfreezing to the surface is not discussed.

4.5 Hara et al. (1995)

Evaluation of test methods of abrasion by ice movements on the surface of reinforced concrete structures

In this study Hara et al. evaluated the characteristics of different test equipment with respect to their suitability in terms of representing abrasion rates of concrete due to moving ice sheets. Some of the tests described in [19] in this section are also referred to in the review [12]. For the sake of completeness for this chapter, the tests are also briefly described herein.

In general, Hara et al. suggest that an ice abrasion apparatus should be able to simulate the following conditions:

- Different contact pressures, ice temperatures and relative velocities.
- Both static and kinetic friction during the same test.
- Easy and accurate measurement of the abrasion amount
- Prevent melting of ice due to frictional heat.
- Allow for easy removal of ice and concrete shavings on the specimen surface.
- The coefficient of friction between ice and concrete must remain constant.
- The test results should be as realistic as possible so they can be used as basis for predicting the wear rate for real structures exposed to ice abrasion.

In order to easier be able to describe and compare the different testing apparatuses, they are divided into the following categories:

- Relative abrasion test
- Revolving disc test
- Tumbler abrasion test
- Sliding contact abrasion test

Relative abrasion test: This test was developed by ABAM Inc together with other companies in the test programme “Developmental Design and Test of High-Strength Light-Weight Concrete Structures in the Polar Ocean Region”, phase I. The apparatus, shown in Fig 4.27, was designed to allow for two cylindrical concrete specimens to be tested simultaneously with an ice contact pressure between 0.21-0.34 MPa while rotating at a speed of 100-500 rpm. The ice block temperature could be varied from 0 °C to -29 °C. The authors emphasize the following weaknesses related to this test:

1. Only kinetic friction acting due to revolution in one direction at constant speed.
2. The relative rotation speed is too high compared with real velocities of moving ice sheets.
3. The slow relative velocity is one of the reasons behind the problem with the ice growth on the concrete surface. It is suggested that the development of frictional heat leads to melting of the ice blocks and hence form the basis for development of an ice film.
4. Due to the wear and tear of the ice blocks during the test, the ice contact area increases, thus reducing the contact pressure. It is therefore not possible to keep a constant contact pressure through the whole test, which is regarded as a significant weakness.

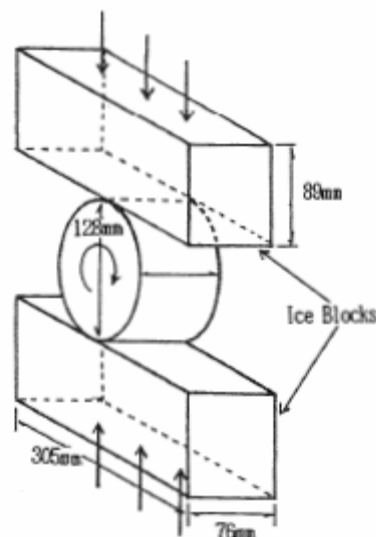


Figure 4.27 Principle sketch of the relative abrasion testing ABAM I [19]

Revolving disc test (i): This test equipment, shown in Fig 4.28, was developed in phase 2 of the ABAM joint industry project and consisted of a hollow, rotating (60 rpm) concrete cylinder with an outer diameter of 300 mm, an inner diameter of 190 mm and a height of 100 mm. A circular ice sheet with diameter 400 mm and thickness 120 mm was pressed towards the end surface of the concrete specimen. The test key parameters can be summarized as follows:

| | |
|------------------------------------|---------------|
| Relative velocity ice/concrete: | 77.0 cm/s |
| Ice temperature: | -15 °C |
| Contact pressure: | 0.45-0.98 MPa |
| Uniaxial compressive strength ice: | 3.5 MPa |
| Sea ice with salt content: | 7-8 % |

The authors underline the following characteristics of the revolving disc test:

1. Only kinetic friction is acting due to revolution in one direction at constant speed.
2. The thickness of the concrete specimen is $(300-190)/2 = 55$ mm, and hence the relative velocity will vary across the cross section of the specimen.
3. As the hollow concrete cylinder penetrates the ice block there is a possibility for undesirable ice growth on the concrete surface.

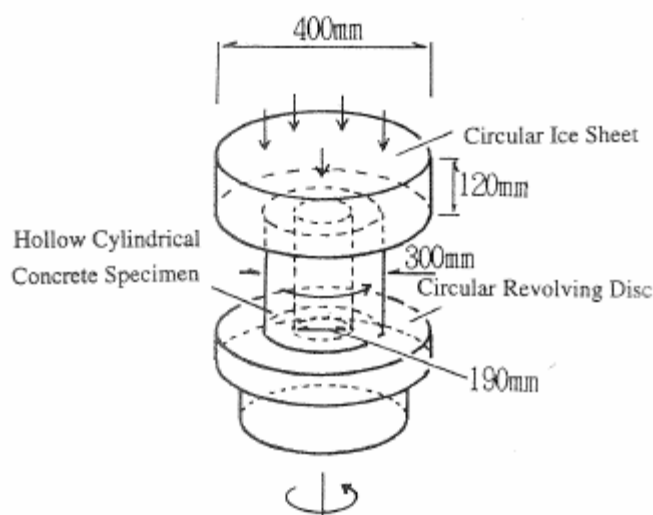


Figure 4.28 Principle sketch of the revolving disk abrasion test [19]

Revolving disc test (ii): This test apparatus was designed and developed by Houvinen et al (1988) of VTT, Finland. Hara et al. describes this as an ice abrasion apparatus with a rotating circular ice sheet. However, according to Huovinen (1990) this is not an ice abrasion apparatus. The test device contains a mechanical cutter that is used to test the concrete wear resistance due to mechanical wear. The apparatus is therefore not described any further in this overview.

Revolving disc test (iii): This test is the so called ASTM C 779 test procedure and it is a general abrasion method. As the test does not deal with ice abrasion it does not fall within the scope of this overview and is therefore not discussed any further.

Tumbler abrasion test: This is another experiment by ABAM and the principle is a rotating cylindrical container with concrete panels/plates mounted on the inner walls. The container is filled with a mixture of ice, coarse aggregates and aluminium oxide grit. The test results are clearly not directly relevant for abrasion caused by ice sheet movements and are therefore left here.

Sliding contact abrasion test (i): This test method was also a part of the ABAM project. The overall concept consists of a vertical concrete specimen travelling back and forth along a 20° arc on the upper face of an ice block, working under an applied vertical stress of approximately 1.7 MPa. The test arrangement is illustrated in Fig 4.29. The technical data of the test can be summarized as follows:

| | |
|--------------------------------|---------------------|
| Diameter concrete specimen: | 76 mm |
| Salinity of ice: | 12 % |
| Contact pressure ice/concrete: | 1.72 MPa |
| Temperature range: | -29 to +2.8 °C |
| Cycle of reciprocation: | 1.75 to 3.5 sec |
| Specimen speed: | 10.1 to 20.2 cm/sec |

According to the authors this apparatus gives a precise representation of the actual phenomena of ice abrasion according to the criteria defined at the start of this chapter. However, some disadvantages are also identified for this apparatus, like when the applied contact pressure is high the concrete specimen tends to penetrate the ice block. In addition, there is a difference in the relative speed across the specimen due to its arc motion leading to an uneven wear rate across the surface. As a last remark it is mentioned that since the abrasion affects the whole end face of the cylinder, there is no surface which can act as a reference surface. The possibility of measuring specimen length was not discussed.

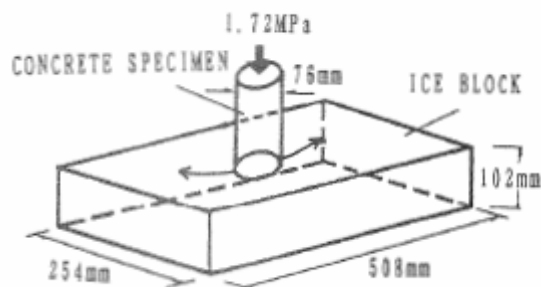


Figure 4.29 Basic concept of the sliding abrasion test [19]

Sliding contact abrasion test (ii): The last test that is described in this summary of different test methods is an apparatus developed by Saeki et al. The machine works by the principle of a horizontal moving trapezoidal concrete specimen interacting with a stationary block of sea ice. Fig 4.30 illustrates the ice-concrete interaction in the sliding contact abrasion test. Technical features of the apparatus read as follows:

| | |
|---|--------------------|
| Width of concrete specimen: | 10 cm |
| Geometry ice block (W x L x T): | (8 x 70 x 8-12) cm |
| Salinity of ice: | 12 % |
| Range of contact pressure ice/concrete: | 0 - 70 MPa |
| Temperature range: | N.A. |
| Specimen speed: | 2, 5, 20 cm/sec |

Test criteria in Table 4.3:

- (1): Allow for changes in ice temperature
- (2): The contact pressure can both be varied and being held constant
- (3): The relative velocity can be varied
- (4): Static and kinetic frictional forces acting alternately during the test
- (5): Allow accurate and easy measurements
- (6): Measures taken against frictional heat and ice melting
- (7): Measures undertaken to remove concrete and ice shavings
- (8): The results must be relevant and useful in predicting real abrasion amounts
- (9): The results can be used as a representative material index for characterization of the ice abrasion resistance for tested material

4.6 Janson (1988)

Long Term Resistance of Concrete Offshore Structures in Ice Environment

In this field study more than 30 lighthouses along the Swedish coast have been studied in order to examine their performance with respect to impact from drifting sea ice. Different types of structural damage were observed but with ice abrasion reported as the most severe. As the lighthouses are spread along the coast they have experienced very different ice and water regimes. This should make it possible to say something about the rate of abrasion related to the ice conditions, unless the different concrete properties are too loosely defined. Both the ice conditions (and other environmental conditions) and the prescribed concrete mixtures used in the lighthouses are described, in order to investigate both the influence of exposure conditions and concrete material parameters with respect to the degree of abrasion.

The inspections were equipped by simple mechanical tools such as hammers, chisels, scrapers and measuring rules. The abrasion depths were measured by using the unabraded surfaces above and below the degraded area as references.

The observed abrasion depths were between 0 and 140 mm, and the tendency was that the depth increased for the lighthouses furthestmost north, where the ice conditions are known to be more severe. The observed results are presented in Fig 4.31 below.

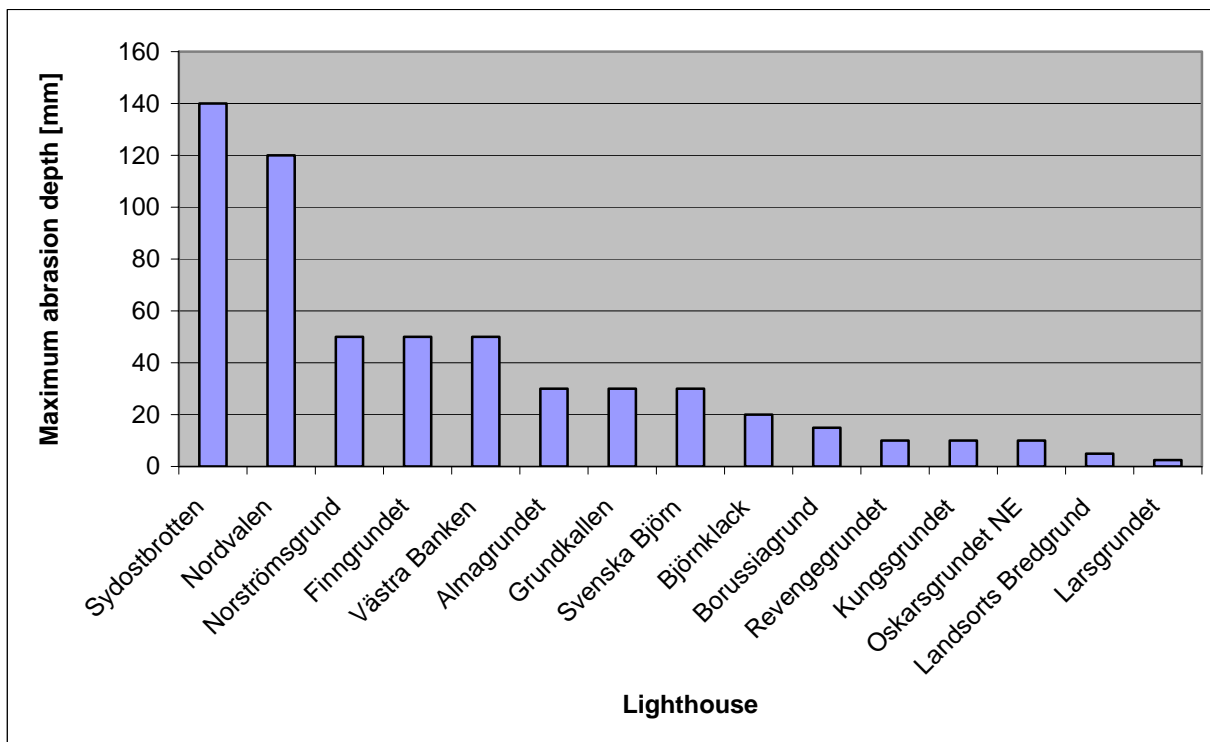


Figure 4.31 – Maximum abrasion depths, lighthouses [5]

The study revealed the following relations between the degree of erosion (abrasion) and exposure conditions:

- No erosion was observed on lighthouses located in areas where the level ice thickness never exceeded 0.3m.
- No erosion of importance has been observed in areas with fast ice throughout the whole winter season.
- Very severe erosion has been detected in areas with close- or open pack ice with ice thickness more than 0.3m.

In order to examine the concrete properties of the lighthouses, drilled-out concrete cores were analyzed by the following laboratory tests:

- Compressive strength
- Tensile strength
- Density
- Cement content
- Chloride content
- Porosity
- Permeability
- Freezing-thawing resistance
- Micro cracks
- Sulphate attack, alkali reactivity and salt crystallization

No erosion of importance has been observed in areas with fast ice throughout the In addition to the ice abrasion, the following deteriorating factors were also briefly discussed with respect to their potential effect on the abrasion resistance of the concrete:

- Freeze-thaw action
- Temperature gradients
- Chemical attacks
- Adfreeze

Without going into details, the above mentioned factors are briefly summarized and discussed with focus on their potential effect on the ice abrasion resistance of the concrete. The study claims that the lighthouses seem to have resisted the freeze-thaw action very well. This is proven by the fact that the major abrasion damages are observed below the water line, where no freeze-thaw action is acting. Temperature gradients are known to cause temperature cracks at the concrete surface. As the temperature gradient above/below water line in the northern Baltic Sea is known to be up to 30 °C or more, it is likely that temperature cracks will occur. As these cracks will be in the macro scale, with unaffected concrete in between, they are not considered to play any major role for the abrasion resistance. In addition, temperature tensile strain does hardly occur below the sea surface ($\Delta T \approx 0$), where most of the abrasion has been observed. When it comes to chemical attacks, laboratory tests of drilled-out concrete cores showed that practically no chemical attack had occurred. No sign of Sulphate attack or any indications of alkali reactions were observed. The adfreeze phenomenon causes ice to accumulate onto the surface of a structure by freezing. If the surrounding ice is drifting, it might cause the bond between the adfreeze ice and the concrete to brake, which in turn could lead to loosening of protruding aggregate particles from the concrete surface. As the most severe abrasion is observed in areas with high ice drift velocity, adfreeze can hardly be a major factor of concern with respect to abrasion. Hence, the study concluded that the above mentioned actions had minimal or no effect on the rate of ice abrasion for the lighthouses.

Local ice forces are limited only by the crushing strength of ice but may be increased by a factor of 3 or more compared to the uniaxial compressive strength due to confinement. The effective strength is also a function of temperature, salinity, grain size and orientation and strain rate. In this study the mechanism behind the phenomenon of ice abrasion is discussed, focusing on the effect of the fluctuating ice pressure acting along the surface of the structure, ref Fig 4.32. The contact pressure is unevenly distributed with distinct peaks that continuously vary in time and space due to the ice indentation. The fatigue effect on the exposed surface followed by this pulsing loading may reduce the strength of the concrete. When the ice pressure locally reaches high peak values, this is believed to cause an abrading effect on the surface. However, no complete compilation of concrete parameters together with corresponding ice abrasion observations was presented to clarify the relation between the material resistance versus the ice exposure conditions.

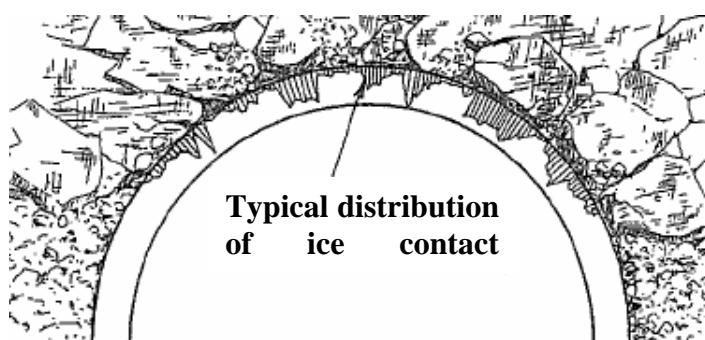


Figure 4.32 Principle sketch of the contact pressure distribution between ice and structure [5]

The loading direction of the attacking ice feature on the surface is also discussed, and found to have an influence on the process causing loosening of aggregate stones. Ice forces acting along the side of a protruding object are considered to be far more severe than a load acting perpendicular to the surface, ref. Fig 4.33. It is particularly underlined the importance of the contribution from the cyclic loading. Both the variation in magnitude and direction of the moving ice significantly reduce the material strength. The differing directions of the attacking ice loads are believed to cause a rocking effect on the aggregate stones which increase the rate of aggregate loss.

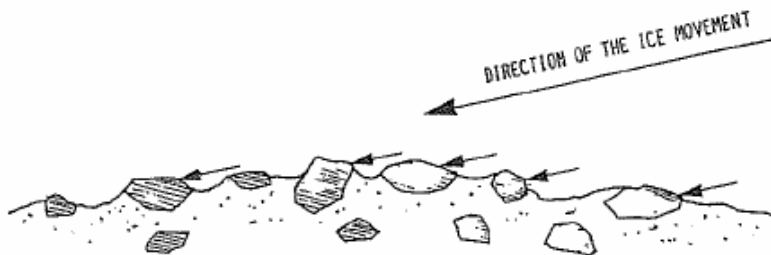


Figure 4.33 Protruding aggregate stones exposed to ice forces from various directions [5]

Abrasion rate for 15 of the examined lighthouses are presented in Fig 4.34.

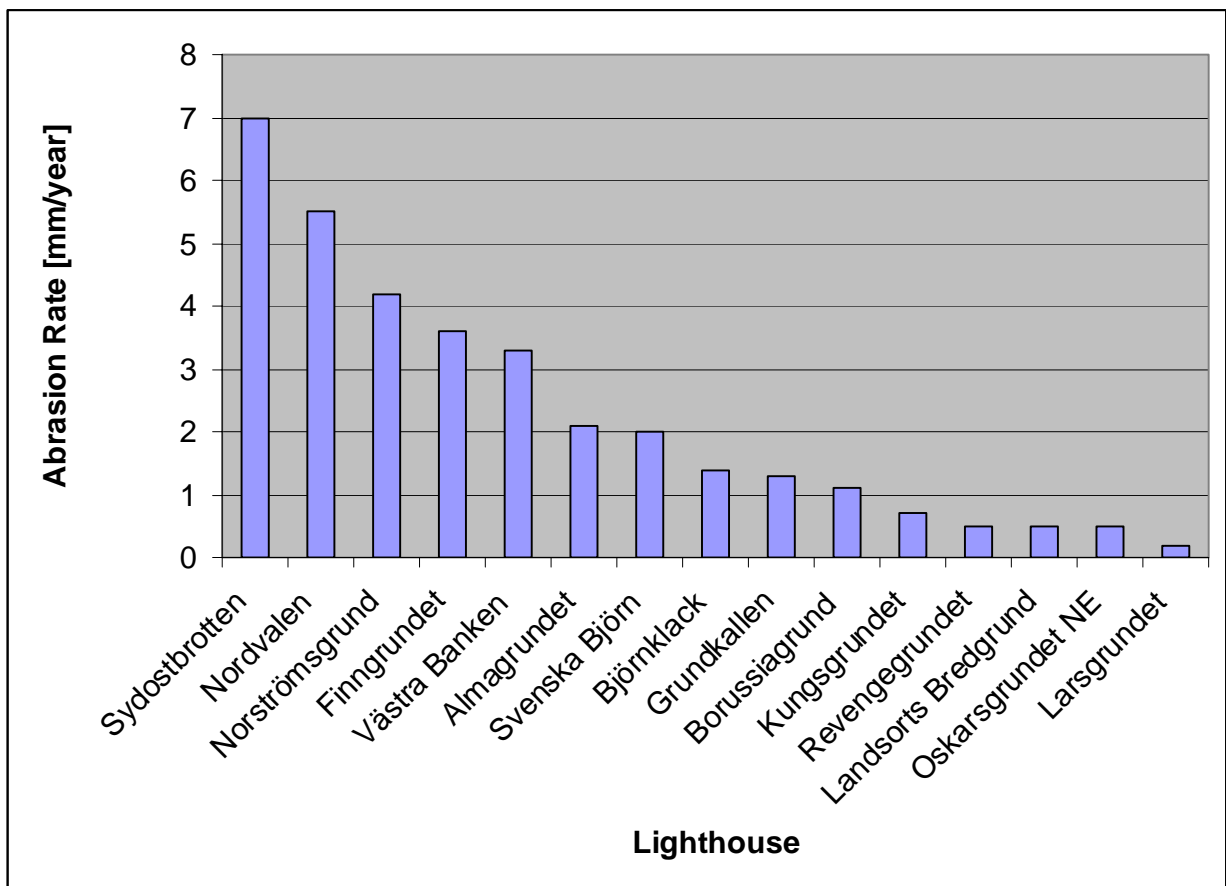


Figure 4.34 Annual abrasion rates, lighthouses [5]

Various ice parameters are evaluated with respect to their effect on the rate of abrasion, and it is found that the ice thickness and ice drift velocity are the two governing. An empirical expression for estimating the abrasion rate was presented [5], Eq. 4-3.

$$\text{Abrasion rate} = \int 0.0015vs dt \quad [\text{mm/year}] \quad (\text{Eq. 4-3})$$

v = ice drift velocity in knots

s = ice thickness in mm

t = time in days

A comparison between Eq. 4-3 and the observed results in Fig 4.34 is shown in Fig 4.35.

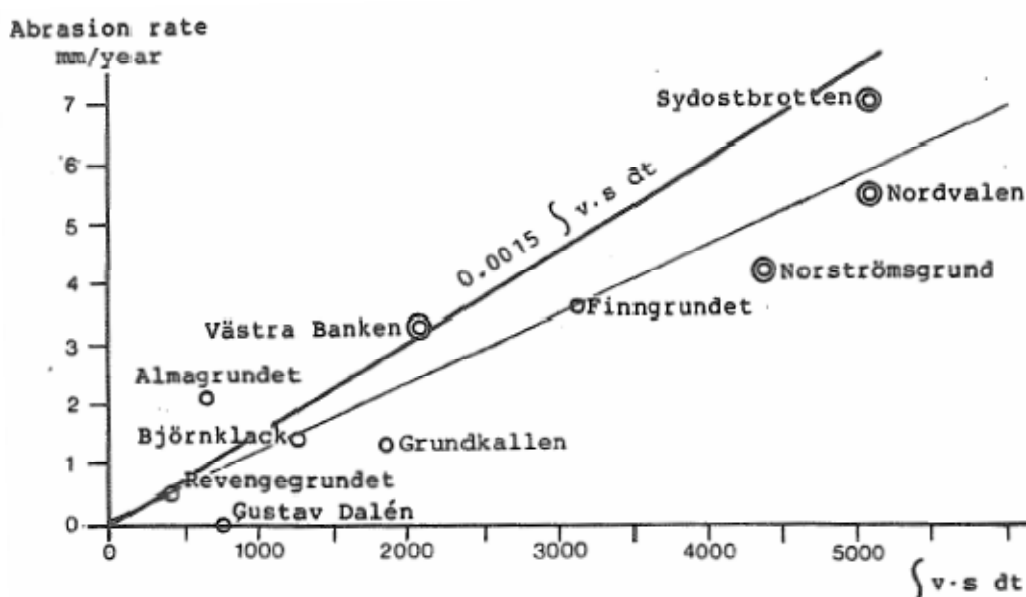


Figure 4.35 Observed abrasion rate as function of $\int vs dt$. [5]

As the salinity in the Baltic Sea is lower than in e.g. Arctic seas, the estimates obtained with Eq. 4-3 is considered conservative. Ice with high salinity contains more brine pockets than ice with lower salinity. A high brine pocket volume reduces the mechanical strength of the ice, and therefore the Baltic Sea ice is generally harder and stronger than Arctic sea ice, at least as far as first year ice is considered. The question of the true mechanism of abrasion is important for the possibility to perform accelerated laboratory tests. Another motivation for gaining more information of the mechanism of ice abrasion is to be able to judge whether other concrete mixes, such as e.g. lightweight aggregate concrete can be used in areas where ice abrasion is a factor of concern.

The formula predicting the expected concrete abrasion presented in this study is limited to concrete qualities with at least the same material quality as prescribed for the lighthouses, ref Table 4.4.

Table 4.4 – Specified material quality concrete, [5]

| f_c | Coarse Aggregate | Fine Aggregate | Cement | Cement Content |
|--------|-------------------|----------------|----------|---------------------------|
| 40 MPa | Naturally Granite | Naturally Sand | Portland | 300-400 kg/m ³ |

4.7 Janson (1989)

Results from the winter seasons 1988 – 1989. Conclusion after the three winters 1986 - 1989. Joint Industry Study, Field Investigation of Ice Impact on Lightweight Aggregate Concrete

A new field study concerning the abrasion problem due to sea ice movement was done over the winter seasons 1986-89. The aim of this study was to directly study the relation between ice conditions and ice impact, and to investigate the resistance against abrasion caused by ice for different types of concrete (particularly lightweight aggregate concrete - LWAC).

The Sydosbrotten lighthouse was selected as the test location i.e. the one with the most abrasion in the previous study of Janson (1988). Ice conditions in this area are severe, and therefore suited the aims of this study well.

In the summer 1986, 24 reinforced concrete panels were installed around the circumference of the caisson wall, ref Fig 4.36.

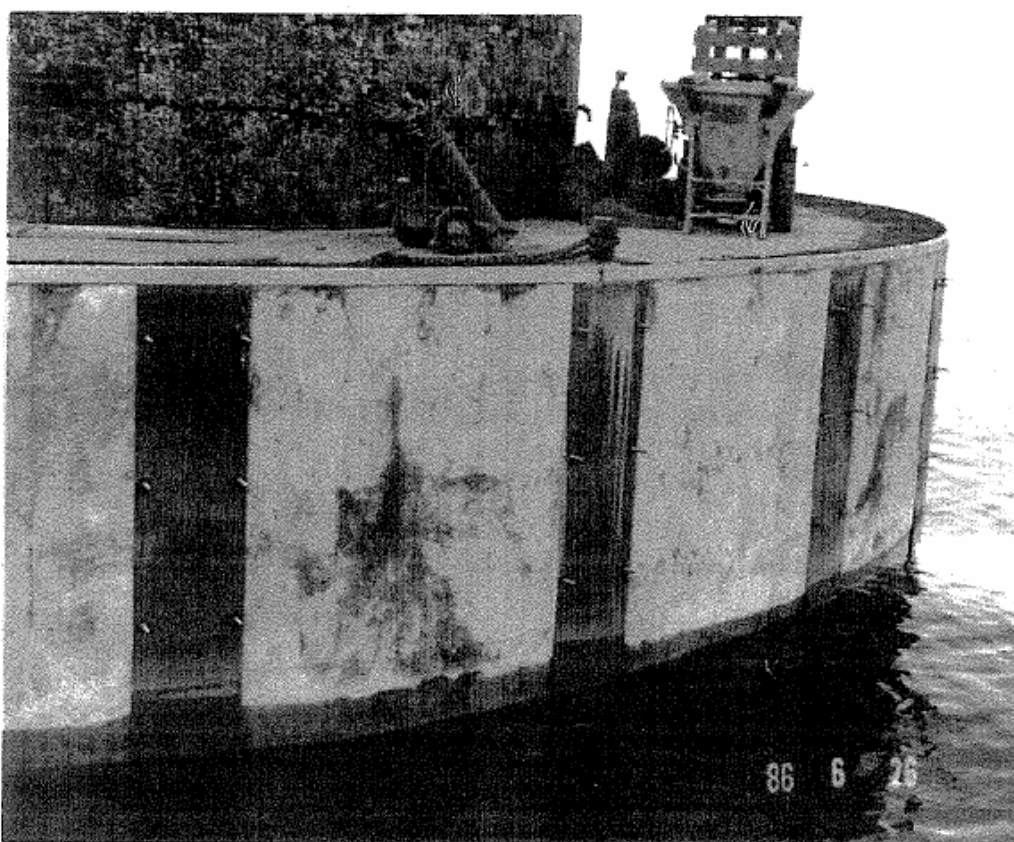


Figure 4.36 Concrete test panels installed at the Sydosbrotten lighthouse [6]

The 24 concrete panels were made of 6 different concrete mixes, 4 panels of each batch. There were 2 mixes of ordinary concrete and 4 mixes of lightweight concrete. The compressive strength of the concretes used varied between 70-90 MPa for the ordinary concrete and between 60-70 MPa for the lightweight mixes (28-days compressive strength). Freeze-thaw tests were also performed for all the concrete batches, and they all showed a good resistance.

In general the dominant ice type in the area is level ice in December and January (mean thickness between 40 and 120 mm), while from February to June it is floes, big and of close ice in the beginning, reduced to small and of open ice in the end of the period (mean thickness varying in the range 110-300 mm).

Actual ice conditions were observed in all three winter seasons, including ice concentration, ice thickness and ice drift. The ice conditions varied significantly during the three winters, and in Table 4.5 the abrasion together with the number of days with ice is presented. The amount of abrasion was measured after each winter season, in the same way as described in Janson (1988).

Table 4.5 – Annual ice abrasion versus ice conditions, [6]

| Winter Season | No. of ice observations (4 times/day) with ice concentrations > 6/10 | Annual average abrasion depth [mm] |
|---------------|--|------------------------------------|
| 1986/87 | 453 | 11.6 |
| 1987/88 | 194 | 3.2 |
| 1988/89 | 17 | 0.3 |

In Fig 4.37 below, Tab 4.5 is illustrated graphically. As seen, the ice abrasion rates vary significantly from year to year pending on the prevailing ice conditions.

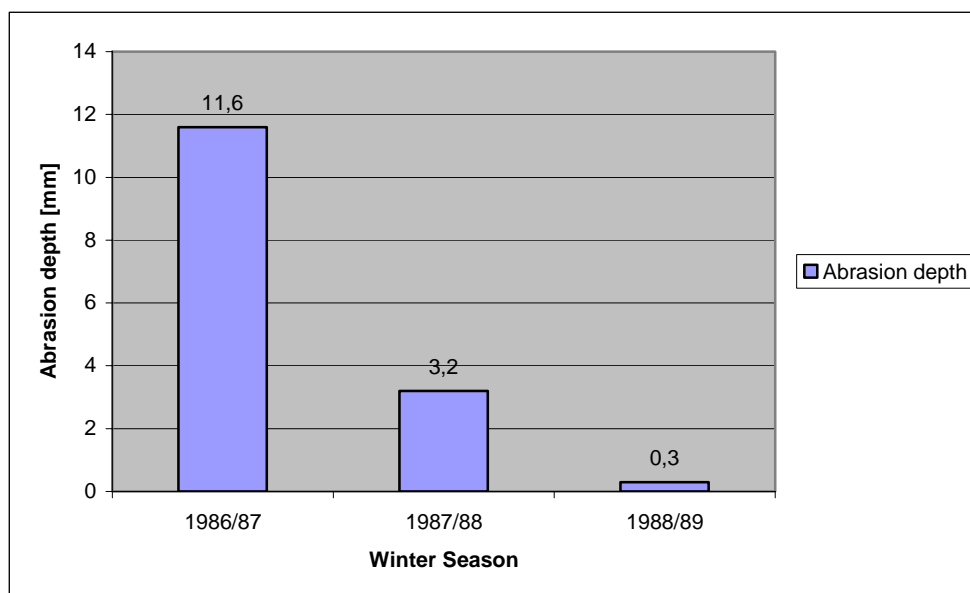


Figure 4.37 Annual ice abrasion at Sydosbrotten lighthouse [6]

The study concluded that variations in ice conditions have a greater influence on the abrasion rates than that of the differing concrete qualities, although the ordinary concrete to some extent showed a modestly higher abrasion resistance compared to the light weight concrete. It was also observed that most of the abrasion occurred at the concrete panels parallel with the dominant ice direction. This implies that ice sliding has a more severe abrading effect on concrete than ice crushing, which occurs perpendicular to the ice sliding direction.

It is assumed that the ice concentration needs to be very high in order for abrasion to occur, as this gives a sufficient high pressure between the ice and the structure. This in addition to the ice thickness and ice strength are considered to be important parameters when evaluating abrasion of concrete by sea ice movement.

4.8 Huovinen (1990)

Abrasion of Concrete by Ice in Arctic Sea Structures

This study, which is the doctoral thesis of Huovinen, comprise investigations of ice abrasion through field observations of light houses, an ice breaker test and laboratory tests of abrasion (without ice) and computer simulations.

Fig 4.38 below shows the three different stages in the mechanism behind ice abrasion on concrete, as they are suggested by Huovinen:

1. Abrasion of cement paste
2. Abrasion of cement paste + loosening of protruding aggregate stones
3. Abrasion of cement paste again after loosening of the protruding aggregate stones

On the right hand side of Fig 4.38 the element mesh of the numerical simulation is shown. It is observed that the mesh is refined in the crucial transition zone between the cement paste and the aggregate stones.

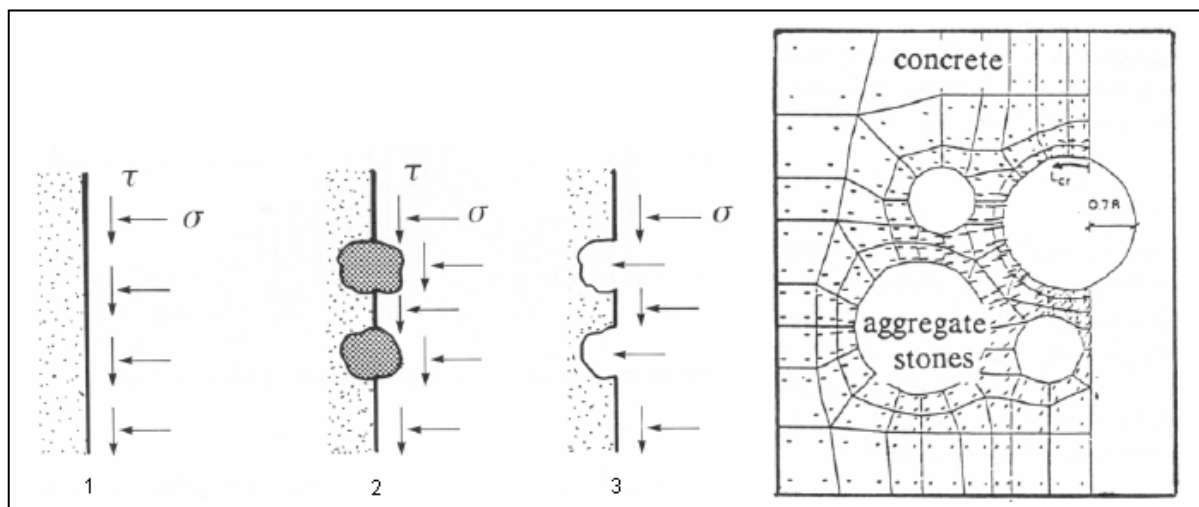


Figure 4.38 Abrasion mechanisms [1]

In the laboratory, the concrete specimens were tested by an abrasion test machine (mechanical cutter) after they had undergone a test regime with varying numbers of freeze-thaw cycles (abrasion testing performed after 0, 25 and 50 cycles). Strength and strain properties of the different concretes were also examined after predefined number of freeze-thaw cycles (0, 5, 25 and 50 cycles).

An extract of the studied concrete mixtures and their performance with respect to (mechanical) abrasion resistance is summarized in Tab 4.6.

Table 4.6 – Abrasion of concrete samples in laboratory (no ice) [1]

| No | Material | f_c [MPa] | w/b | Exposure | Abrasion (mechanical) |
|----|----------------------|-------------|------|---|-----------------------|
| 1 | ND Concrete | 60 | 0,27 | Freeze-thaw (50 cycles) + abrasion (mechanical) | 6,2 |
| 2 | ND Concrete | 60 | 0,28 | | 5,4 |
| 3 | ND Concrete | 60 | 0,31 | | 9,3 |
| 4 | ND Concrete | 40 | 0,41 | | 10,8 |
| 5 | ND Concrete | 40 | 0,36 | | 9,1 |
| 6 | ND + Silica Concrete | 60 | 0,31 | | 2,6 |
| 7 | ND + Silica Concrete | 60 | 0,31 | | 4,8 |
| 8 | LW Concrete | 30 | 0,35 | | 11,2 |
| 9 | LW Concrete | 30 | 0,35 | | 11,5 |
| 10 | ND Slag Concrete | 60 | 0,29 | | 4,5 |
| 11 | ND Slag Concrete | 60 | 0,29 | | 7,1 |

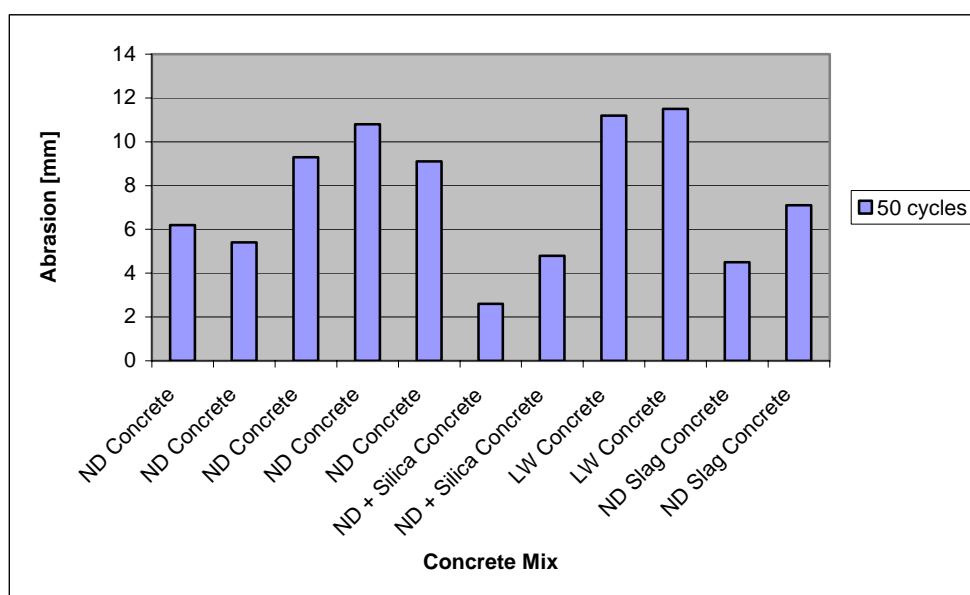


Figure 4.39 Abrasion performance of concrete samples in laboratory after 50 freeze-thaw cycles [1]

As seen, use of cement replacements like silica fume and blast furnace slag had a positive effect on the abrasion resistance. The lightweight (LW) concrete experienced the highest degree of abrasion among the different specimens. It should be noted that the LW concrete also had the lowest compressive strength (30 MPa) amongst the tested material samples.

In the icebreaker tests a concrete specimen was mounted in the bow of an icebreaker as shown in Fig 4.40.

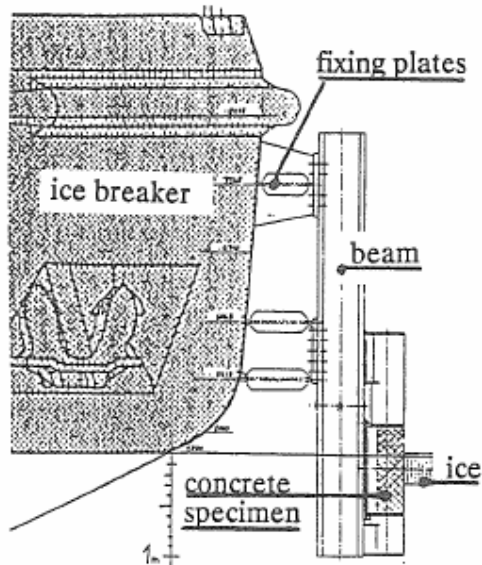


Figure 4.40 Icebreaker test arrangement. [1]

After a travelling distance of about 40 km in the front of an icebreaker, the mean abrasion depths varied from 2-15 mm while the corresponding maximum values ranged from 7-30 mm. The best abrasion resistance was achieved by the blast furnace slag cement concrete and the lowest resistance was observed for the lightweight concrete, ref Fig 4.41 below. The tendency from the icebreaker test is consequently well correlated with the results from the laboratory testing.

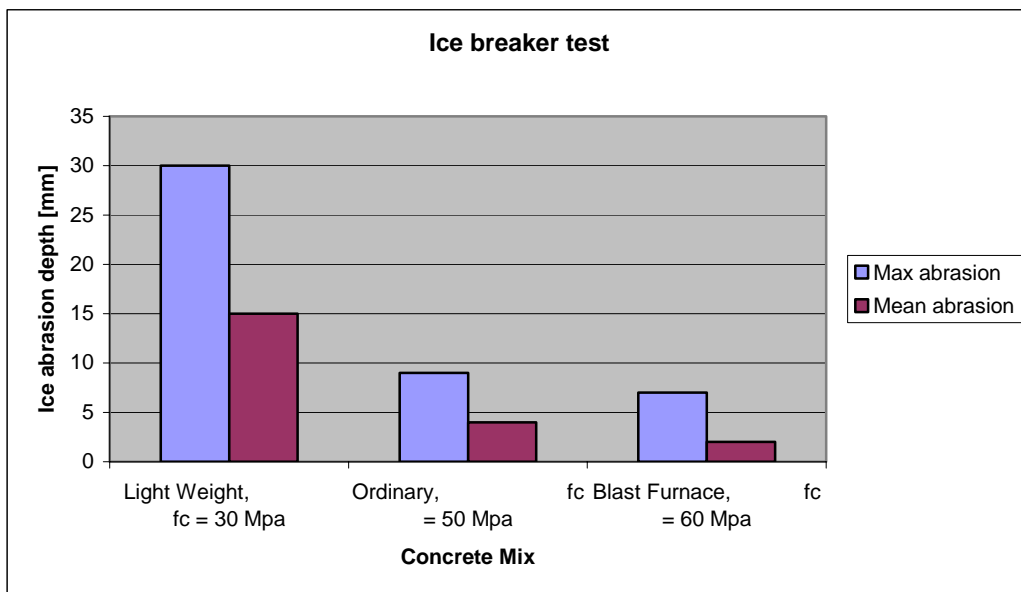


Figure 4.41 Ice abrasion results from the icebreaker test [1]

Four different lighthouses in the Gulf of Bothnia were also examined, all caissons with a circular cross-section, constructed in the period 1963-65, all with air-entrained concrete of strength class K40. The measured, mean abrasion depth of the lighthouses after 22-24 year of exposure varied in the range 22-39 mm, and the maximum abrasion depth observed was 56 mm, ref Fig 4.42. The compressive strength at the water level was in the range 35-46 MPa, and in the range 65-80 MPa at 1.5 m above the water level, ref Fig 4.43. The reduced compressive strength at water level is caused by deterioration of the concrete due to repeated freeze-thaw cycles.

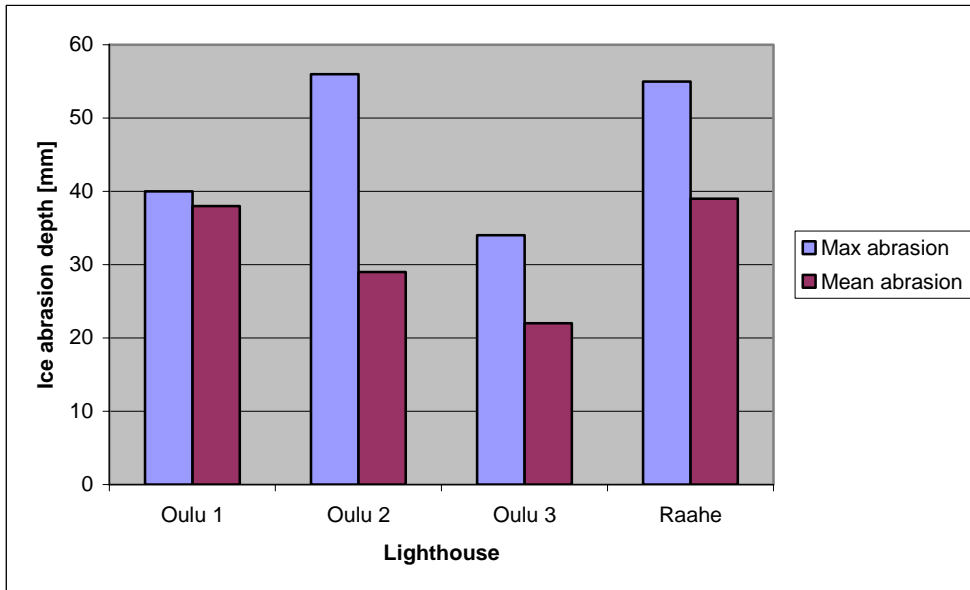


Figure 4.42 Ice abrasion depths observations for lighthouses in the Gulf of Bothnia [1]

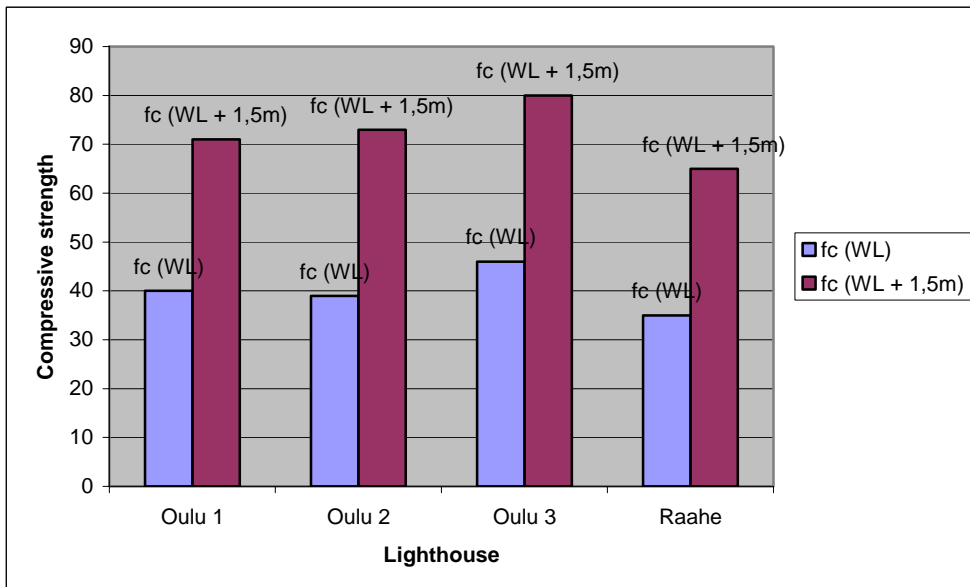


Figure 4.43 Compressive strength for lighthouses in the Gulf of Bothnia at Water Level (WL) and 1,5m above WL (WL + 1,5m), [1]

An abrasion diagram developed from the numerical calculations is presented in Fig 4.44, valid for a normal distribution of the aggregate particles, when the tensile strength is at least 10 % of the concrete compressive strength, and the bond strength between aggregate particles and cement paste is at least 90 % of the concrete tensile strength.

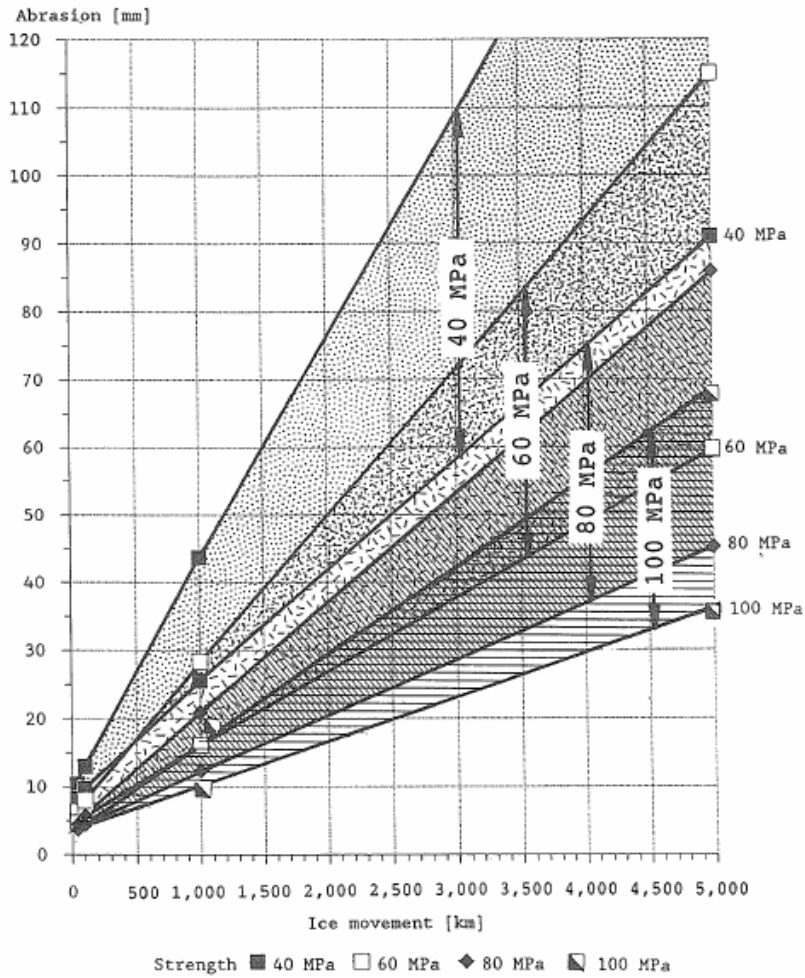


Figure 4.44 Abrasion of concrete [mm] ($f_c = 40, 60, 80,$ and 100 MPa) as a function of ice sheet movement [km] based on numerical simulations [1]

A comparison of the abrasion obtained with the different test methods is given in Fig 4.45.

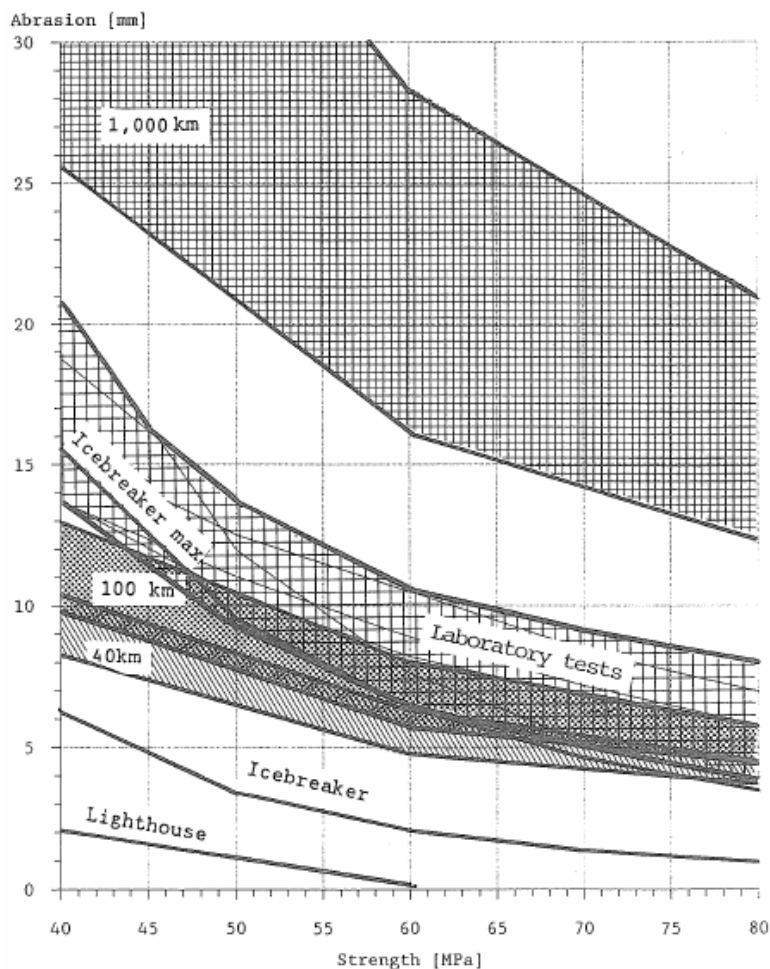


Figure 4.45 Ice abrasion as a function of concrete compressive strength [1]

The following main conclusions were listed from this study:

- The most important mechanical factor of the concrete with respect to resistance against ice abrasion is the compressive strength, which should be at least 70 MPa to secure a good resistance against abrasion.
- The concretes with water/cement ratio no higher than 0.30-0.35 showed a good resistance against abrasion.
- Normal weight concretes containing silica fume and blast furnace slag showed both a higher strength and a higher abrasion resistance than lightweight concrete with blast furnace slag.
- Increasing the maximum size of the aggregates also contribute to an increase in the abrasion resistance of concrete.
- The local ice loads acting on protruding aggregate stones are considerably greater than the uniaxial compressive strength of the ice.

4.9 Hara et al. (1995)

Prediction of the degree of abrasion of bridge piers by fresh water ice and the protective

The authors of this field study (F. Hara et al.) have studied field ice abrasion on one bridge pier in Japan. They also suggest a calculation method for predicting abrasion rates.

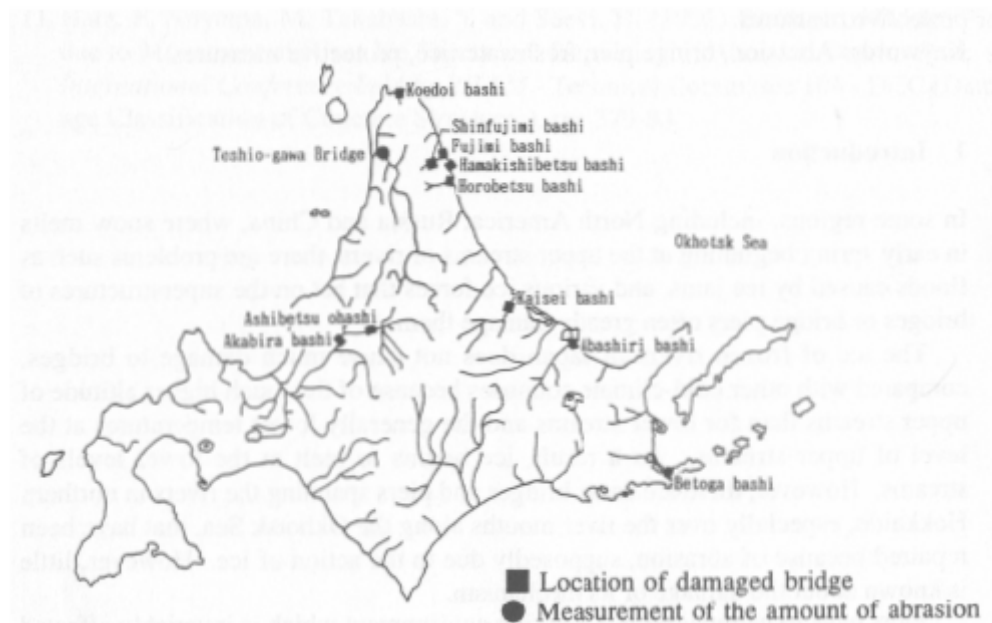


Figure 4.46 – Locations of damaged bridges [20]

Several damaged bridges located near the river mouths along the Okhotsk Sea (known to freeze completely during winter) were identified ref Fig 4.46. The maximum ice thickness in the rivers where the damaged bridge piers are observed varies between 30 and 50 cm. The findings of the field study are summarized below:

1. The ice abrasion rate is largest at the waterline.
2. Most abrasion was observed on the upstream side of the bridge piers.
3. Maximum abrasion rate observed was in the range of: 1.0 – 5.0 mm/year.
4. Abrasion rates increases with increasing ice velocity and pressure.
5. For the most severe conditions the ice abrasion had resulted in exposure of the reinforcement bars.
6. There seemed to be more severe abrasion for the bridge piers located in rivers with a lake or a swamp upstream or downstream.

Fig 4.47 shows the cross section of the evaluated pier (Teshio-gawa Bridge) and the average abrasion depth at four locations along the periphery of the pier. It is observed that the highest abrasion depth is found in point 2, i.e. approximately halfway between 0° and 90° when the flow direction is defined as 0°.

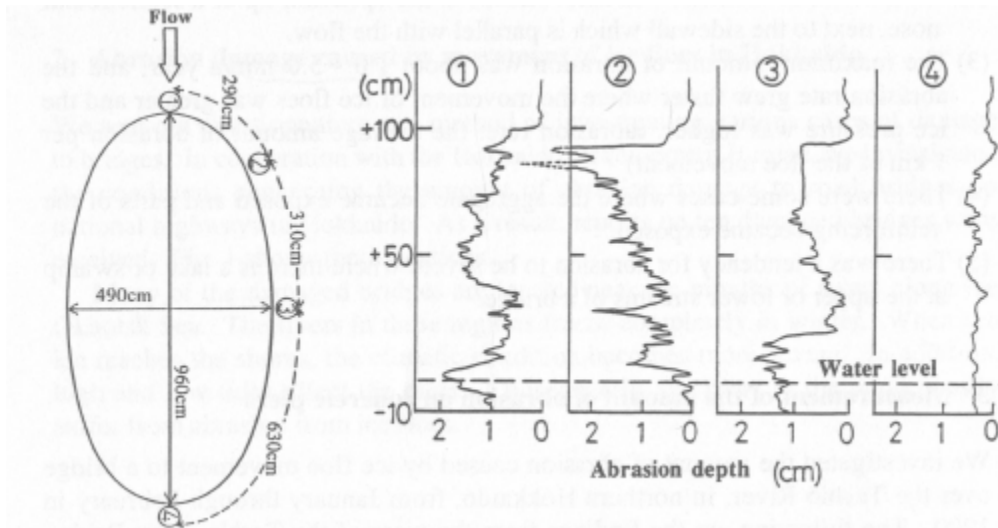


Figure 4.47 – Cross section of bridge pier and corresponding abrasion depth [20]

The authors suggest the following expression to estimate abrasion rates based on one concrete quality and ice-condition:

$$\text{Abrasion rate: } S = 0.0012 \cdot \sigma_v \tag{Eq. 4-4}$$

where,

S = abrasion rate [mm/km]

σ_v = ice contact pressure [kgf/cm²]

$-10\text{ }^\circ\text{C} \geq T \geq 0\text{ }^\circ\text{C}$

When equation Eq. 4-4 is compared to actual field data it overestimates the abrasion depths. This is probably due to the fluctuations in the water levels. The authors suggest that it should be safe to assume average abrasion depths of only one half of the estimated values from Eq. 4-4. In Fig 4.48 estimated, average abrasion rates versus ice temperatures are plotted for different ice contact pressures.

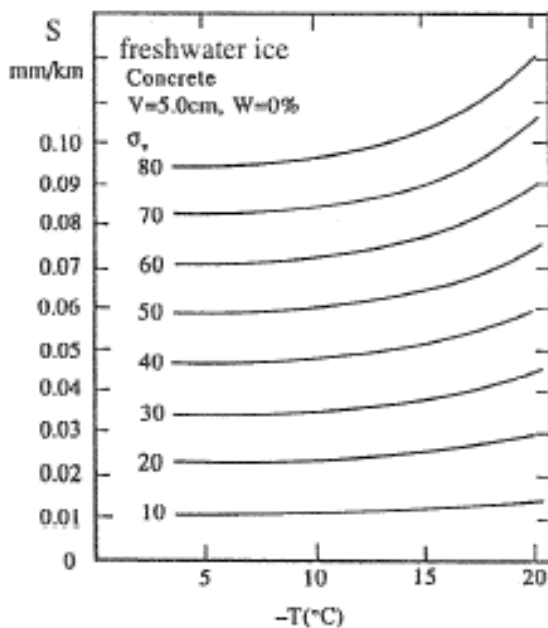


Figure 4.48 – Estimated average abrasion rates versus ice temperatures [20]

Concluding on the field measurements on ice abrasion on a single bridge pier, the authors underline the importance of the ice temperature, the contact pressure, the structural diameter and the concentration of sand etc within the moving ice. Based on the limited available data in this study, the results is probably most suitable for comparison with other field studies like e.g. [5, 6, and 1] to evaluate difference in ice abrasion rates for different materials under varying ice conditions. From Tab 3.1 it is seen that the observation [20] is somewhere close to a median value of the lighthouse study [6].

4.10 Malhotra et al. (1996)

Manufacture of Concrete Panels, and Their Performance in the Arctic Marine Environment

The aim of this Canadian study was to investigate the performance of concrete panels in the Arctic marine environment. 12 panels were installed at a site at Nanisivik (latitude 73° North), Baffin Island, North West Territories, Canada, Fig 4.49.



Figure 4.49 Location of Nanisivik, Baffin Island [3]

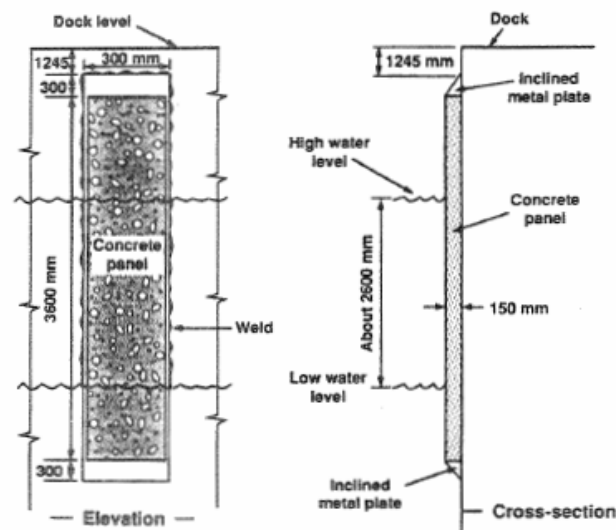


Figure 4.50 Concrete panels as they were mounted in the dock at Nanisivik [3]

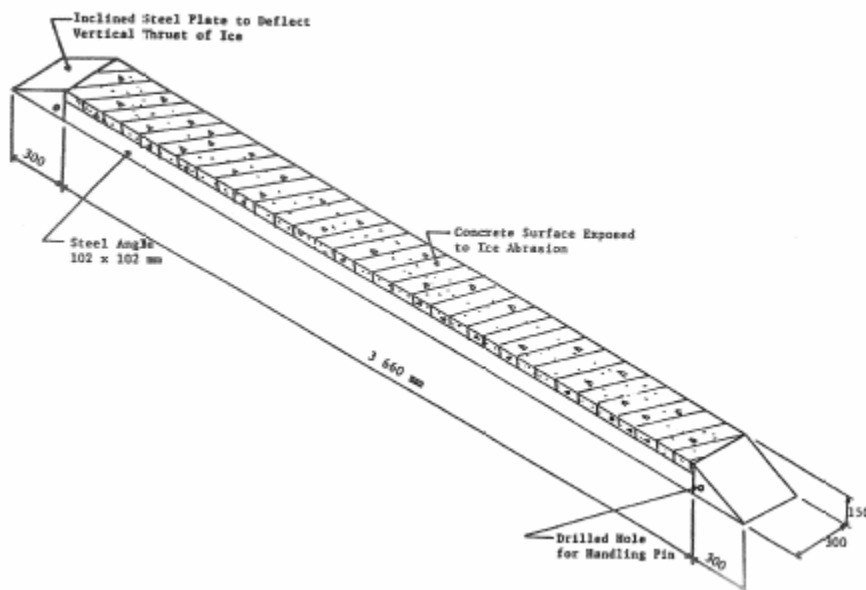


Figure 4.51 Isometric view of the concrete test panels [3]

The panels were installed in a way that secured that the upper part of each panel always was above high water level, while the lower part always was below low water level.

12 different concrete mixes were used in the study. The following description was given: “Six of the mixtures contained about 50 kg/m³ steel fibre, while the remaining were of plain concrete. Crushed limestone aggregate was used for six of the concrete mixtures, and expanded shale lightweight aggregate was used for the rest. The effects of fly ash (20 %), silica fume (10 %), slag (50 %), and a combination of fly ash (20 %), and silica fume (10 %) as cement replacements (by volume) in concrete were also investigated. Air content in hardened concrete were in the range 4,5 – 6,5 % for normal-weight concrete and between 4,0 – 6,5 % for the lightweight concrete.

Detailed information regarding the materials used, the concrete mixtures, casting of the test panels, and the properties of the concretes are given, and briefly the 28-days compressive strength for the normal-weight concrete was in the range 40 – 55 MPa, about 37 – 45 MPa for the lightweight concrete, and the water/cement ratio ranged from 0.37 to 0.42. Incorporating 50 % slag as the cement replacement had a positive effect on the compressive strength of the concrete.

Table 4.7 – Concrete properties [3]

| Mix. No. | Cementitious Materials | Fibres | f_c [MPa] | w/b ratio |
|----------|---------------------------|--------------|-------------|-----------|
| 1 | ND ref | Plain | 38 | 0.40 |
| 2 | ND ref | Steel fibres | 42 | 0.40 |
| 3 | ND + 10% silica | Plain | 42 | 0.40 |
| 4 | ND + 10% silica | Steel fibres | 49 | 0.40 |
| 5 | ND + 50% slag | Plain | 51 | 0.40 |
| 6 | ND + 50% slag | Steel fibres | 52 | 0.42 |
| 7 | LWA + 20% fly ash (fa) | Plain | 35 | 0.37 |
| 8 | LWA + 20% fly ash (fa) | Steel fibres | 37 | 0.37 |
| 9 | LWA | Plain | 41 | 0.39 |
| 10 | LWA | Steel fibres | 42 | 0.40 |
| 11 | LWA + 10% silika + 20% fa | Plain | 39 | 0.38 |
| 12 | LWA + 10% silika + 20% fa | Steel fibres | 43 | 0.39 |

The resistance of abrasion of the investigated concretes was tested according to the standard abrasion test ASTM C 779 Procedure C”, and the results are shown in Fig 4.52 and 4.53. It is seen that the use of steel fibres especially has a positive effect on the abrasion resistance.

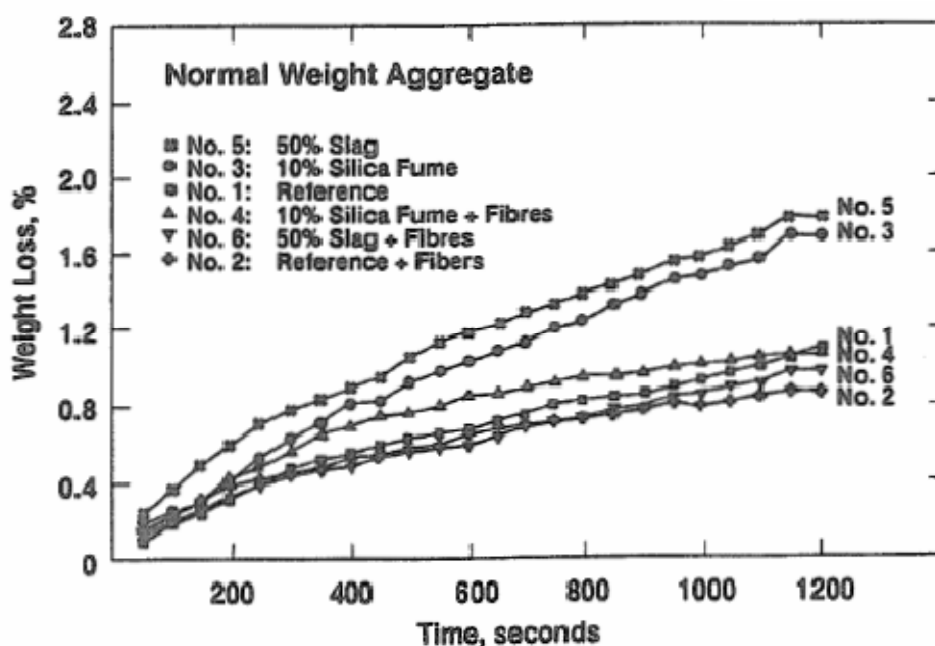


Figure 4.52 Resistance to abrasion (ASTM C779) of the normal-weight concrete [3]

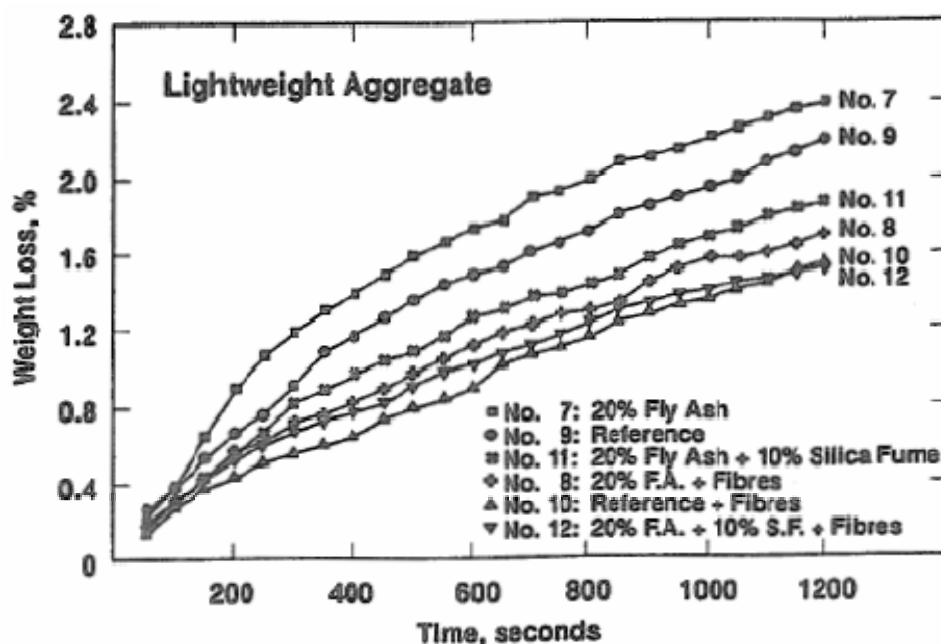


Figure 4.53 Resistance to abrasion (ASTM C779) of the lightweight concrete [3]

No description of the ice conditions are given, but it is stated that the test panels have experienced; “very severe exposure which included freezing and thawing cycles, ice abrasion, ice impact, and sea water attack”.

It was concluded, after both visual and micro structural examination, that the concrete test panels after seven years of exposure in extreme exposure conditions were in good to excellent conditions. It was observed some local corrosion of the steel fibres for the fibre-reinforced concrete panels.

4.11 Fiorio et al. (2002)

Experimental study of the friction of ice over concrete under simplified ice–structure interaction conditions

This study describes ice-structure interaction at the centimetre scale and comprises small scale cyclic friction testing between micro-concrete (i.e. concrete with average roughness between 0 and 0.6 mm) and laboratory grown freshwater ice. The experimental results are presented in terms of friction coefficients. Available material data for both ice and concrete are summarized below.

- Ice properties: Laboratory grown S2 columnar freshwater ice ($D_{\text{grain}} = 8$ mm) grown from deionized water.
- Geometry ice specimen (cylinder): Diameter: 60 mm, Height: 96 mm
- Contact pressure ice/concrete: 0.25 – 0.80 MPa
- Ambient temperature: - 10 °C (+/- 0.5 °C)
- Concrete specimen: Concrete plates 175x150 mm with average roughness between 0 and 0.6 mm
- Aggregate size: 0.2 – 5 mm
- Sliding velocity: 1.67×10^{-6} – 1.67×10^{-4} m/s

The friction tests were performed with a shear box apparatus, originally designed for soil mechanics experiments, ref Fig 4.54. The concrete plate was mounted on top on a carriage which moved horizontally below the ice cylinder along a 30 mm stroke. The driving speed was held constant during each test. The velocity range lied between 10^{-6} and 10^{-4} m/s and involved five different driving speeds within this range. The columnar ice grains were placed with the axis parallel to the concrete surface and hence perpendicular to the direction of the frictional force. The normal and tangential forces were measured with two spring-like dynamometers. Two linear displacement transducers were used to record the normal and tangential displacements. Prior to the tests, the average roughness of each concrete plate was measured. The tests regime involved two different loading scenarios, i.e. either a constant load test (CLT) or a level load test (LLT).

Under the CLT the concrete specimen slid for at least ten cycles (each cycle 30 mm) under a constant ice load for all cycles. During the LLT a series of twelve successive cycles were performed with increasing (first six cycles), then decreasing (last six cycles) ice loading. The ice load/pressure, ranging from 0.025 – 0.8 Mpa, were kept constant within each cycle. Before the LLT, the concrete specimens were exposed to five cycles with a ice pressure of 0.5 MPa in order to reach a stable level of friction.

Fig 4.55 shows typical friction curves for the above mentioned test regimes within CLT and LLT. After the end of each test, the concrete specimen underwent optical microscopy measurements. The results of these observations gave information on the physical mechanisms involved in friction.

In Fig 4.56 and 4.57 the evolution of tangential stress versus tangential displacement is shown for the CLT. As seen the “steady state” coefficient of friction is reached after approximately 5-7 cycles for a given sliding velocity. During the initial, transitory regime, the level of friction increase before it reaches a steady state value. The increase in friction during these first cycles is associated with the increase of the real area of contact between ice and concrete, and is caused by the gradually penetration by the asperities of the concrete into the ice. This mechanism is time dependent and believed to be caused by the visco-plastic behaviour of ice.

As seen in Fig 4.55 and 4.56 each half-cycle starts by a peak friction value (“sticking peak”) caused by an adhesive bond between ice and concrete when the sliding motion is stopped, i.e. at the end points where the sliding speed shift direction. The breaking of this adhesive bond is ductile for low sliding velocities and brittle for high velocities. It is not quantified in which velocity range the response shift from ductile to brittle behaviour. Furthermore the authors mention that within some velocity ranges the tests experienced stick-slip motions, but this phenomenon was not defined as a scope of the paper and was therefore not investigated any closer.

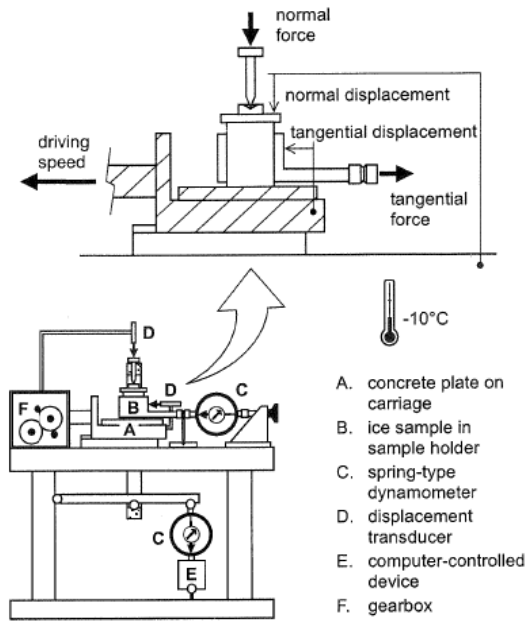


Fig 4.54 Test arrangement (friction apparatus)

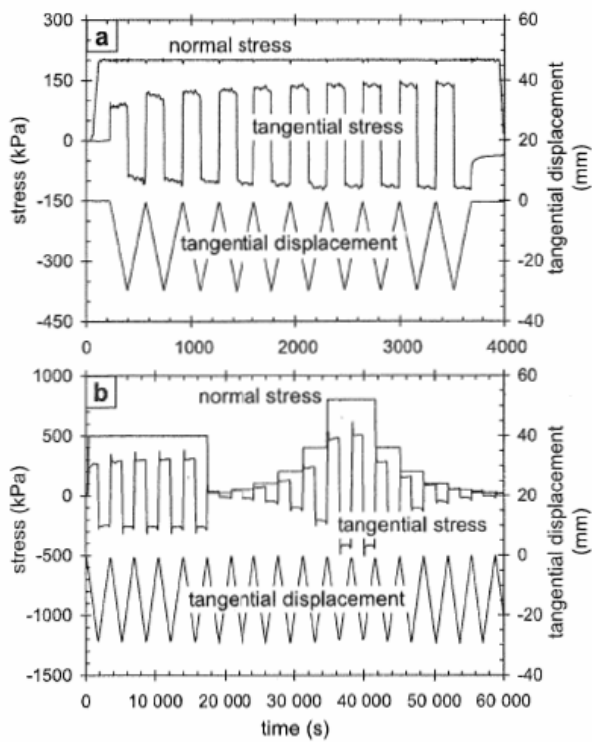


Fig 4.55 Typical friction curves for CLT (a) and LLT (b)

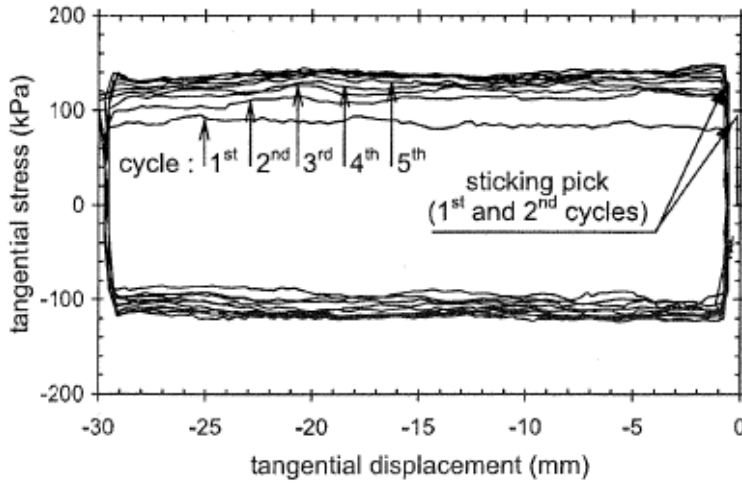


Fig 4.56 Evolution of friction during CLT

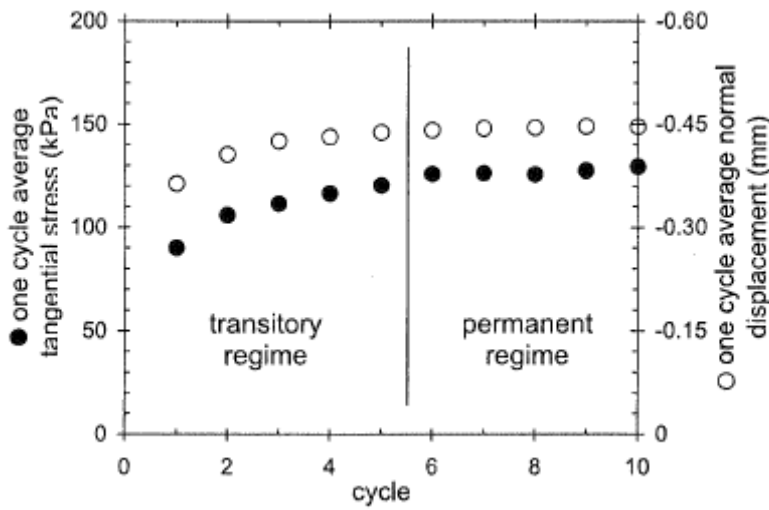


Fig 4.57 Transitory versus steady state friction regime

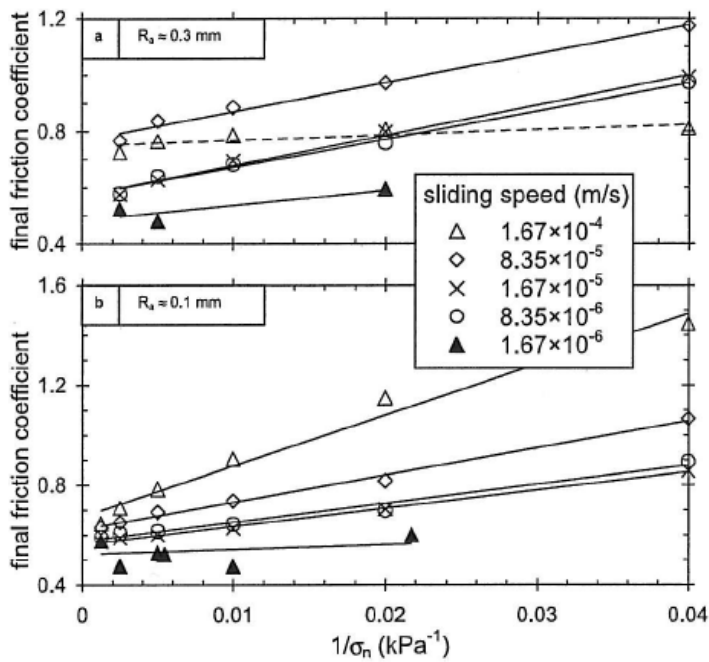


Fig 4.58 Normal stress versus steady state coefficient of friction

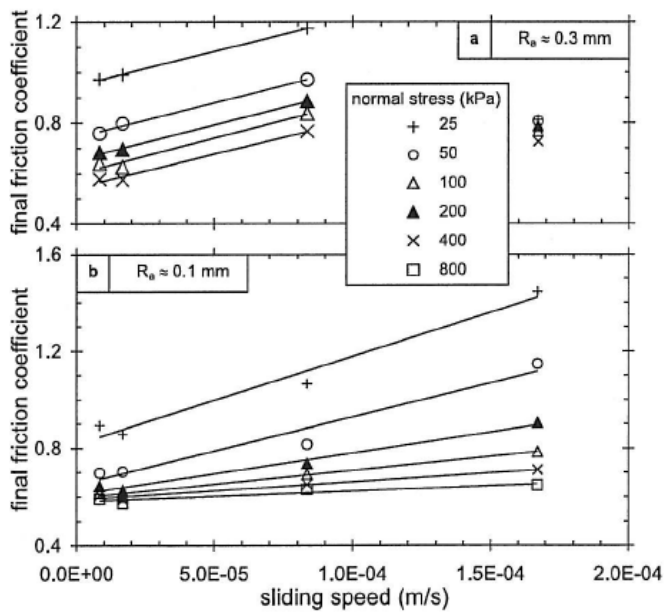


Fig 4.59 Sliding velocity versus steady state coefficient of friction

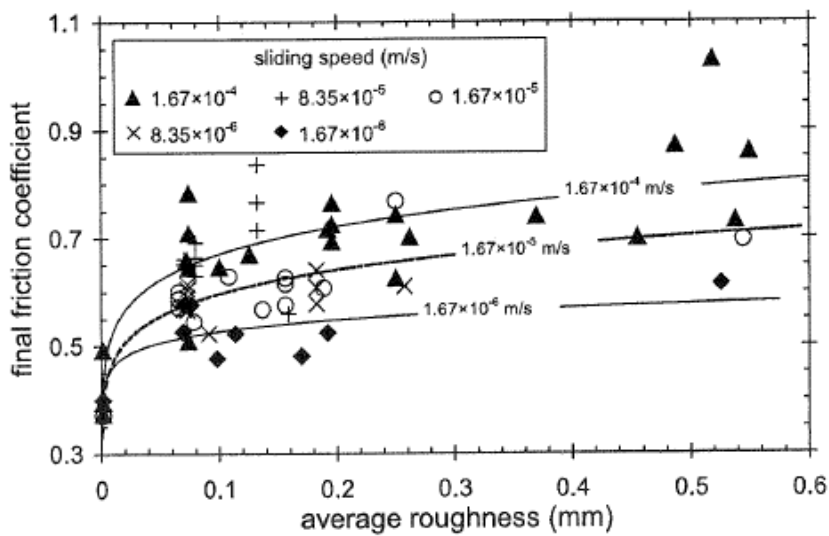


Fig 4.60 Effect of average roughness on the steady state coefficient of friction

The effect of the ice sliding velocity and of the average roughness on the steady state coefficient of friction suggests that, in the range of velocity considered here ($1.67 \times 10^{-6} - 1.67 \times 10^{-4}$ m/s), friction of ice over concrete is mainly governed by the visco-plastic properties of the ice. For a given normal stress and sliding velocity, friction is an increasing function of average roughness. The effect of the sliding velocity on friction is also explained from the viscoplasticity of ice. An increase in the sliding velocity leads to an increase in the strain rate of the ice around the protruding aggregates and hence an increase in the tangential stress and thereby of friction. The influence of the normal stress (“contact pressure”) on friction cannot be explained from the ice viscoplasticity properties. However, the experimentally observed increase of the friction coefficient with the inverse normal stress is typical for friction with adhesion at the contact surface. For this case, the tangential stress does never reach zero, even for negligible values of normal stress.

It is known from ice-ice and ice-metal experiments that sintering of the ice is responsible for high values of adhesion. Adhesion of 1 MPa should be easily achieved between ice and concrete, due to adsorption of water molecules around the cement particles. At low normal stresses adhesion is therefore the main mechanism behind friction, which then appears as the tangential stress needed to break the adhesive bond.

The experimental results in this study reveals that the two main physical mechanisms responsible for friction, within the contact conditions used in this study, are viscoplasticity of ice and ice-concrete adhesion. The viscoplasticity-dependence explains the influence of the sliding velocity and the average roughness on the coefficient of friction. On the other side, adhesion seems to be the main contributor at low normal/contact stresses. As this study focus on friction testing under varying roughness, contact pressure and sliding velocity it is not emphasized on any description of the concrete properties (like e.g. w/c-ratio, compressive strength, etc).

4.12 Fiorio (2005)

Wear characterization and degradation mechanisms of a concrete surface under ice friction

This paper focus on small-scale effects of the friction-induced wear of micro-concrete based on experiments with cyclic friction and wear tests in conjunction with optical observations and topographic measurements. Available material data for the ice and concrete samples are summarized below.

- Ice properties: Laboratory grown S2 columnar freshwater ice ($D_{\text{grain}} = 8 \text{ mm}$) grown from deionized water.
- Geometry ice specimen (cylinder): Diameter: 60 mm, Height: 90 mm
- Contact pressure ice/concrete: 0.25 – 0.80 MPa
- Geometry concrete specimen: 15x150x175 mm
- Cement: Portland CEM I 42.5
- Aggregate: Fine sand (0.2 – 0.6 mm), coarse sand (3 – 5 mm)
- Cylinder compressive strength: $f_c = 24.8 \text{ MPa}$
- w/c = 0.6

Two different types of concrete batches have been tested; plates with roughness 0.28 mm and smooth plates with roughness 0.11 mm, ref Fig 4.62. The simplification introduced by use of micro-concrete is justified as the grain size is considered representative with respect to structural concrete near its surface, where large size aggregates are known to be under-represented.

The ice-concrete friction experiments were performed with a direct shear box apparatus as shown in Fig 4.63 and as previously described in Fiorio et al 2002. It is emphasized that the cylindrical ice sample holder was placed with a gap of 1 mm above the concrete surface in order to avoid physical contact between the sample holder and the concrete surface. The normal stress was imposed through a lever, which was operated by a computer controlled electro-mechanical device. In order to trace the development of the ice abrasion process, a series of measurements by use of optical microscopy techniques were performed after each test. These observations made the basis for analyzing the physical mechanisms involved in friction and wear.

Optical observations of the ice and concrete specimens showed formation of a layer of finely crushed ice and cement together with the fine sand particles at the surfaces, ref Fig 4.64. Qualitative observations of the abrasion process revealed a progressive wear of the cement paste and the fine sand particles. At the end of the friction testing series, a groove formation in the sliding direction was observed.

Fig 4.65 shows the evolution of the frictional wear for the smooth plates with roughness 0.11 mm. The observed wear is a result of two phenomena; a general wear that is gradually and uniformly distributed over the frictional area, and a so called catastrophic wear limited to local areas. The catastrophic wear represents a sudden ejection of coarse aggregates from the surface layer. The phenomenon occurs when aggregate-cement paste bond has been sufficiently weakened by the abrasion of the cement paste. Thus it is clear that catastrophic wear happens as a consequence of general wear.

From Fig 4.66 it appears that the general wear occurs in two stages. The initial stage corresponds to the wear of the superficial layer of cement paste and the rate is dependent upon the roughness of the concrete plate. The permanent or steady state stage is characterized by a lower rate of abrasion which is independent of the roughness of the concrete surface. With respect to general wear it is measured an abrasion rate of 20 mm/km in these experiments. This is significant higher than what is observed in other comparable studies, and is by the authors believed to be caused by the use of small sized aggregates in the micro concrete.

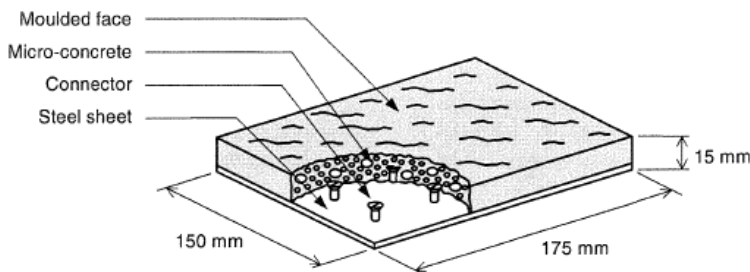


Fig. 1. Configuration of the concrete plate.

Fig 4.61 Geometry of concrete specimen

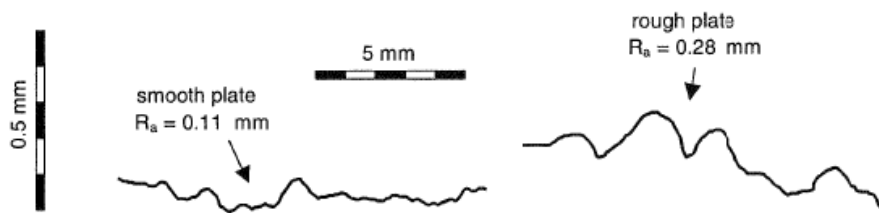
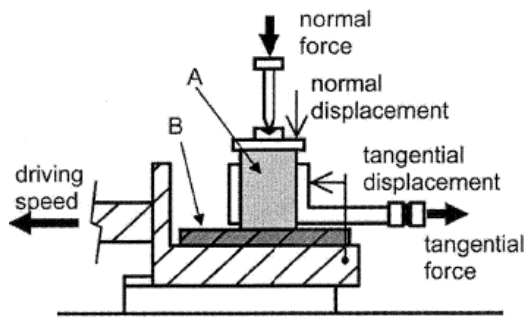


Fig. 2. Typical geometry of the surface of the smooth and rough concrete plates.

Fig 4.62 Smooth and rough surface topology of concrete specimen



- A. concrete plate on carriage
- B. ice sample in sample holder
- C. spring type dynamometers
- D. displacement transducers
- E. computer controlled device
- F. gearbox

Fig 4.63 Experimental set-up

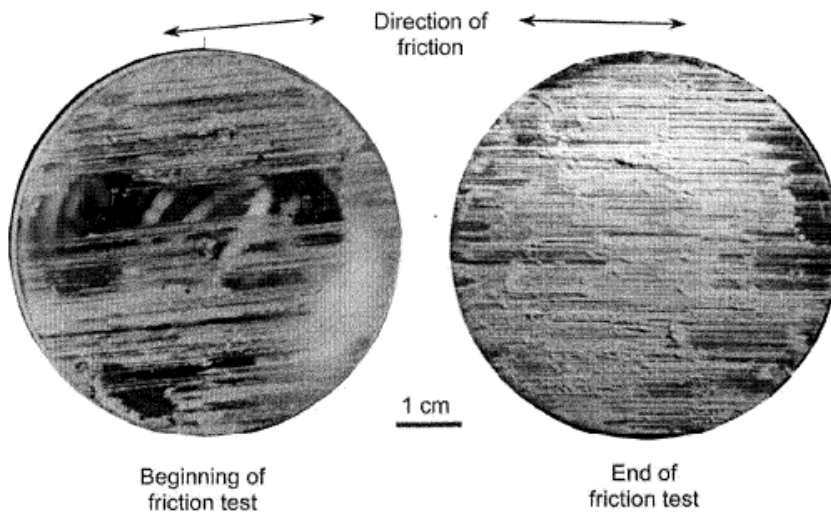


Fig. 6. Wear particles at the ice surface after friction on concrete.

Fig 4.64 Wear particles at the ice surface

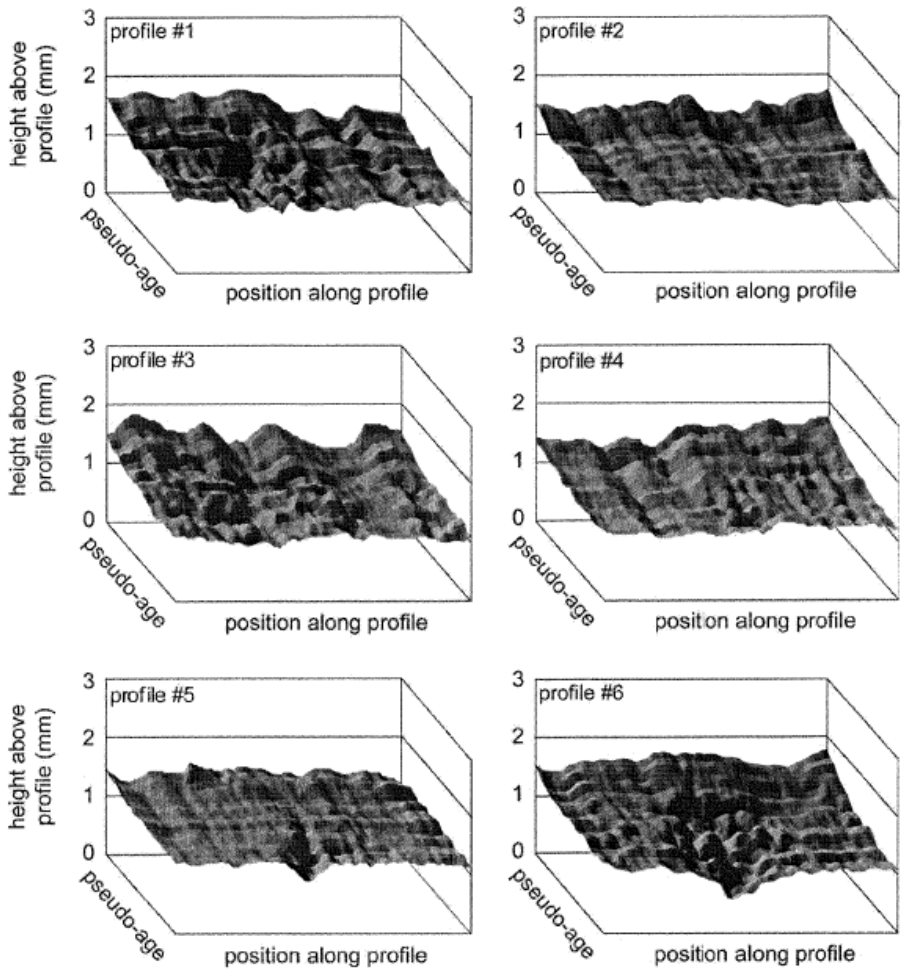


Fig 4.65 Topographic evolution of the smooth concrete plate due to ice friction

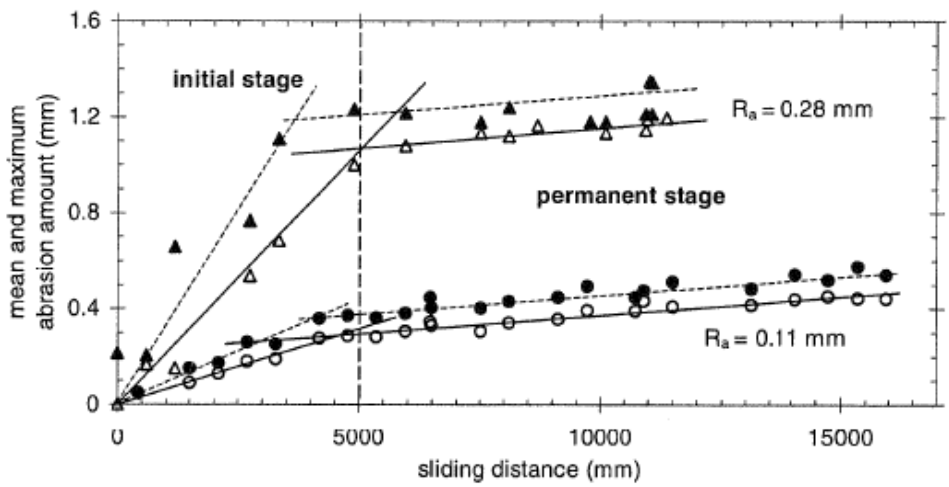


Fig 4.66 Max (black) and mean (white) ice abrasion rates versus ice sliding distance

5 FINAL DISCUSSION

Several abrasion test methods have been launched to evaluate the performance of both normal weight and lightweight concretes developed to resist wear from ice loads on marine structures. The test results from the different studies are not always well correlated as seen in this overview. This may partly be due to the fact that the phenomenon ice abrasion is a more complex matter than purely the frictional force between the two materials of ice and concrete. One should also keep in mind that the material parameters of both concrete and ice separately, are not easily predicted. When studying the interaction between the two of them together, it is not surprising that the results sometimes are somewhat scattered. In addition to testing in laboratories it is also important to establish long-term field tests to monitor the abrasion effect in full scale, including logging of key parameters such as e.g. ice drift, -velocity, -temperature, salinity, porosity, compressive strength, etc. In the same way it is equally important to log the concrete parameters such as, compressive strength, tensile strength, w/c ratio, air content, use of additives, etc. A complete picture based on all these parameters cannot be found in the reviewed data.

As seen in the previous chapters, various field- and laboratory studies have been carried out to find a method to estimate ice abrasion rates. These tests have been performed with different test equipment and with emphasize on different parameters with respect to e.g. abrasion method, contact pressure, temperatures, ice drift velocity, etc. A direct comparison of the individual test results is therefore generally not possible, as the results appear to be influenced by the applied test method. However, some of the tests provide comparative results on the effects of some material variables on ice abrasion, like e.g. concrete compressive strength, type of aggregate and properties of the cementitious binder materials. The majority of the reviewed tests do not account for freeze-thaw effects or other deteriorating factors known to act in severe marine environments. The results from the various laboratory tests should perhaps more often have been followed up by parallel field experiments in order to check the correlation with respect to the ice abrasion performance.

In the majority of the ice abrasion studies presented in this overview, the significance of the ice conditions is emphasized, with ice temperature and contact pressure as the two most essential. Several of the tests show little or no difference of the wear resistance for different concrete qualities. Exceptions are Hanada (rock) and Huovinen (concrete) who both concluded that the ice abrasion resistance was improved by increasing the material compressive strength. Huovinen also found positive effects on the wear resistance of concrete by increasing the maximum aggregate size, reducing the water/cement (w/c) ratio, using normal density aggregates instead of lightweight aggregates and use of cement replacements such as blast furnace slag and silica fume. Furthermore, he suggests a uniaxial compressive strength of minimum 70 MPa and a w/c ratio in the range of 0.30-0.35 to ensure what he defines as a “good abrasion resistance”. As a contradistinction to the findings of Huovinen with respect to abrasion resistance of lightweight aggregates versus normal aggregates a mechanical abrasion test (ASTM Method with revolving discs) by the ABAM Engineers Inc. reports on the opposite. However, the latter was not an ice abrasion test and hence the results are therefore not directly comparable.

Both the tests by Itoh et al. and Huovinen concluded that the abrasion process can be divided into three distinct stages or regions with one wear rate corresponding to each of the three phases. After the two initial, transient phases, the third region is characterized by a constant abrasion rate and is therefore named the “steady state” region. These observations indicate that the concrete surface has an influence on the abrasion; thus the concrete properties do have an effect on the wear rate. In the expression for estimation of ice abrasion proposed by Huovinen, the concrete uniaxial compressive strength is suggested used as the single concrete parameter.

Interaction with other deteriorating mechanisms (frost, de-icer salt, abrasion by other solids than ice) will complicate the deterioration process more, ref. Jacobsen et. al [16]. It is therefore suggested to concentrate on a study on ice abrasion where only the concrete material- and ice load parameters are varied. Introduction of other deteriorating forces should preferably be done in cooperation with other durability studies, for example in some sort of round-robin test with partial exposure at varying labs.

Common for the studies presented herein is that they all show signs of ice abrasion on the concrete, despite of significant difference in test conditions both with respect to ice- and concrete properties. There is, however one exception, and that is the field investigations by Malhotra et al. (1996), where no abrasion were observed after seven years of exposure in a dock in Nanisivik, Baffin Island, Canada. The study does not give any detailed description of the ice conditions, except that the concrete test panels experienced “very severe exposure”, including freezing and thawing cycles and ice abrasion. It is therefore difficult to say anything explicit about the relation between concrete abrasion and ice conditions for that study. One explanation might be that the concrete panels experienced primarily ice crushing and less ice sliding, where the latter presumably generates the most surface wear due to ice confinement and friction. The concrete compressive strengths of this study was maximum 55 MPa (28-days) which is relatively modest compared to some of the other studies, which had compressive strengths up to 90 MPa and still experiences abrasion.

Some of the considered field studies that are described herein are located in the Gulf of Bothnia, and comprise both Swedish and Finnish lighthouses. These show varying degree of damage from abrasion, and both ice conditions and concrete properties are concluded to influence on the rate of abrasion. It was observed wear rates ranging from 0 to 7 mm/year. The northernmost lighthouses, which experienced the most severe ice conditions, showed the highest abrasion rates. However, this work did neither contain sufficient detailed information on the concrete material and its potential effect on the observed ice abrasion rates. The study by Huovinen is the only work that clearly concludes that the compressive strength of the concrete is one of the key parameters governing the abrasion resistance of the material. Huovinen clearly presents the properties of the concrete in detail in his work. In none of the other studies considered herein the concrete properties are described and investigated to the same extend as in his work. This might perhaps be the reason for the somewhat different conclusions of Huovinen (1990) compared to the other studies. However, Huovinen (1993) also concluded that: “The lower the temperature of the ice and the higher the stress intensity, the greater is the abrasion”, which coincides well with the conclusions in the other studies.

Although some studies conclude that the ice abrasion rates of concrete are not dependent on the material parameters, it has not according to the author’s knowledge been carried out any ice abrasion tests for ultra high strength concrete, i.e. compressive strength beyond approximately 150 MPa. Some of the most severe abrasion rates covered in this document is based on concretes with relatively low compressive strengths and often without any air entrainment. Concrete samples of e.g. the lighthouses in the Gulf of Bothnia shows significant lower compressive strength of the concrete near the waterline compared to samples taken some meters above. This implies that the concrete has weakened in the crucial abrasion zone. It would therefore be of special interest to see the abrasion performance of an ultra high strength concrete reinforced with fibres, perhaps also with aggregate stones with small grain size to minimize surface roughness, in a field experiment.

Finally, some of the studies like e.g. Itoh et al. (1988 & 94) study the effect of reducing the coefficient of friction between the ice and concrete surface by a low frictional coating. In e.g. steel hulls for ice breakers there is widely use of low friction coatings. Similar coatings might also be applied to concrete surfaces, but the risk of water accumulation behind them, and corresponding chipping/spalling, has so far been a show stopper for the use of coating in environments with freeze-thaw action. With water trapped behind the coating, combined with freezing and thawing, it is troublesome to document a coating lifetime of 30 years, in order to guarantee a maintenance-free surface for e.g. a sub-arctic offshore structure.

6 CONCLUSIONS

The phenomenon of concrete abrasion due to sea ice movement is complex, involving different mechanisms and parameters. From the previous studies on the subject there have been somewhat scattered conclusions, and various methods of estimating the rate of abrasion have been proposed. In general it seems that:

- The rate of abrasion increases with increasing ice contact pressure and decreasing ice temperature
- Ice sliding cause more abrasion than ice crushing
- The ice abrasion is reduced with increasing material strength as observed in laboratory tests on rock and field tests combined with modelling of concrete
- Using cement replacements like silica fume and blast furnace slag has shown a positive effect on the amount of abrasion

It is important to obtain sufficient insight on the effect of both ice conditions (load) and concrete parameters (resistance). Ice parameters should be monitored separately (ice-, thickness, velocity, sliding distance - km/year, mechanical properties, etc) in field versus laboratory experiments under controllable conditions (ice-, sliding velocity - cm/s, pressure/load characterization, coefficient of friction, salinity/porosity and its effect on ductility and friction, temperature, etc). A wide range of concrete parameters should then be investigated (compressive- and tensile strength, cement replacements, aggregate type/distribution/size, bond between aggregate and cement paste, w/c ratio, use of fibres, use of ultra high performance concrete (UHPC), characterization of the concretes responds to freezing alone (i.e. length change). This will lead to more reliable prediction on how efficiently special materials like for example ultra high performance concrete can be used to protect against ice abrasion.

Additionally, general studies on abrasion (not only ice), mechanisms and relation to other parameters such as strength, aggregate properties, -bond etc should be reviewed. Available equipment for ice abrasion and possible developments such as e.g. use of ice cubes in a sliding test should be evaluated for use in concrete ice abrasion testing.

As there probably will be a high construction activity in the sub arctic areas in the years to come, a model predicting the expected concrete abrasion as precisely as possible, would be of great interest and should be one of the aims in future studies.

7 REFERENCES

- [1] Huovinen, S., (1990) "Abrasion of concrete by ice in arctic sea structures", VTT Publications 62, (Doctoral thesis), Espoo, 110 p, app. 31 p.
- [2] Huovinen, S (1993). Abrasion of Concrete Structures by Ice. Cement and Concrete Research, Vol. 23, No. 1, 1993. Pp 69-82.
- [3] Malhotra V.M., Zhang M.H., Sarkar S.L., (1996) Manufacture of concrete test panels, and their performance in the arctic Marine Environment, 3rd CANMET/ACI Int.Conf.Perf. of Concr. Marine Environm., Spec.Vol Odd E.Gjørv Symposium, Ed.P.K.Mehta p. 55-81
- [4] Sandwell (B. Maddock) Technical Memo TM 107 Sakhalin II, Phase II Project Facilities Design (2002)
- [5] Janson, J. E. (1988). Long Term Resistance of Concrete Offshore Structures in Ice Environment. 7th International Conference on Offshore Mechanics and Arctic Engineering. Houston, Texas, 7-12 Feb. 1988. New York 1988, American Society of Mechanical Engineers. Vol. III., pp. 225-231.
- [6] Janson, J. E. (1989) Report No. 3, Results from the winter season 1988 - 1989, Conclusion after the three winters 1986 - 1989. Joint Industry Study, Field Investigation of Ice Impact on Lightweight Aggregate Concrete, VBB.
- [7] B. Fiorio. (2005) Wear characterization and degradation mechanisms of a concrete surface under ice friction, Construction and Building Materials Volume 19, Issue 5, p. 366-375.
- [8] B. Fiorio, M. Meyssonier and M. Boulon, (2002) Experimental study of the friction of ice over concrete under simplified ice–structure interaction conditions, Can. J. Civil Eng. (9) p. 347–359.
- [9] B. Fiorio. (2005) Wear characterization and degradation mechanisms of a concrete surface under ice friction, Construction and Building Materials Volume 19, Issue 5, p. 366-375.
- [10] Saeki et al, Consec 1995 Sapporo
- [11] Nawwar, A.M., Malhotra V.M., Development of a Test Method to Determine the Resistance of Concrete to Ice Abrasion and/or Impact American Concrete Institute SP 109 (1988) 401-426
- [12] G. C. Hoff, Resistance of Concrete to Ice Abrasion – A Review, American Concrete Institute SP 109 (1988) p. 427-455
- [13] Malhotra, V.M., Zhang, M.H., and Sarkar, S.L. (1996) Manufacture of Concrete Panels, and Their Performance in the Arctic Marine Environment. Odd E. Gjørv Symposium on Concrete for Marine Structures, an integral part of the Third CANMET/ACI International Conference on Performance of Concrete in Marine Environment, St. Andrews-By-The-Sea, New Brunswick, Canada, August 4-9, 1996, pp. 55-81.
- [14] Itoh, Y., Yoshida, A., Tsuchiya. M., Katoh, K., Sasaki, K., and Saeki, H. (1988) An Experimental Study on Abrasion of Concrete Due to Sea Ice. Presented at the 20th Annual Offshore Technology Conference in Houston, Texas, May 2-5, 1988. (OTC 5687), pp. 61-68.
- [15] Itoh, Y., Tanaka, Y., and Saeki, H. (1994) Estimation Method for Abrasion of Concrete Structures Due to Sea Ice Movement. Proceedings of the Forth (1994) International Offshore and Polar Engineering Conference, Osaka, Japan, April 10-15, 1994, Vol. II, pp. 545-552.
- [16] Jacobsen, S., Sistonen, E., Huovinen, S., Marchand, J., and Tremblay, M.H. (2006) Abrasion and Scaling of Concrete by Ice, Studded Tires and Frost-Salt: Interaction and Service Life Modeling. Proc. Advances in Concrete through Science and Engineering, RILEM PRO 51 ISBN 2-35158-003-6, Québec, Canada, Sept.11-13 (2006) 23 p.
- [17] Hanada, M., Ujihira, M., Hara, F. and Saeki, H. (1996) Abrasion Rate of Various Materials Due to the Movement of Ice Sheets. Proceedings of the Sixth (1996) – International Offshore and Polar Engineering Conference, Los Angeles, USA May 26-31, 1996

- [18] Gerwick, B. C., (1983) Artificial Islands for Arctic Offshore Exploratory Drilling and Production Islands, University of California, Department of Civil Engineering, Berkeley, California
- [19] Hara, F., Takahashi, Y. and Saeki, H., Evaluation of test methods of abrasion by ice movements on the surface of reinforced concrete structures, Proceedings of the International Conference on Concrete under Severe Conditions, CONSEC '95 Sapporo, Japan, Vol 1 pp. 475-484
- [20] Hara, F., Saeki, H., Sato, M., Takahashi, Y. and Tachibana, H., Prediction of the degree of abrasion of bridge piers by fresh water ice and the protective measures , Proceedings of the International Conference on Concrete under Severe Conditions, CONSEC '95 Sapporo, Japan, Vol 1 pp. 485-494
- [21] "ABAM Engineers Inc., Developmental Design and Testing of High-Strength Lightweight Concretes for Marine Arctic Structures, Program Phase I, Joint Industry Project Report, AOGA Project No. 198, Federal Way, Washington, May 1983"
- [22] "ABAM Engineers Inc., Developmental Design and Testing of High-Strength Lightweight Concretes for Marine Arctic Structures, Program Phase II, Joint Industry Project Report, AOGA Project No. 230, Federal Way, Washington, May 1983"
- [23] "ABAM Engineers Inc., Developmental Design and Testing of High-Strength Lightweight Concretes for Marine Arctic Structures, Program Phase III, Joint Industry Project Report, AOGA Project No. 230, Federal Way, Washington, May 1983"